*Inorg. Chem.* **2006**, *45*, 10613–10628


# Ag(I) and Cu(II) Discrete and Polymeric Complexes Based on Single- and Double-Armed Oxadiazole-Bridging Organic Clips

**Yu-Bin Dong,* Ting Sun, Jian-Ping Ma, Xia-Xia Zhao, and Ru-Qi Huang**

*College of Chemistry, Chemical Engineering and Materials Science, and Shandong Key Lab of Chemical Functional Materials, Shandong Normal University, Jinan 250014, P. R. China*

Received July 6, 2006

Four new oxadiazole-bridging ligands (**L1**–**L4**) were designed and synthesized by the reaction of 2,5-bis(2-hydroxyphenyl)-1,3,4-oxadiazole with isonicotinoyl chloride and nicotinoyl chloride, respectively. **L1** and **L3** are unsymmetric single-armed ligands (4- or 3-pyridinecarboxylate arm), and **L2** and **L4** are symmetric double-armed ligands (4- or 3-pyridinecarboxylate arms). Nine new complexes, [Ag(**L1**)]$PF_6$·$CH_3OH$ (**1**), [Ag(**L1**)]$ClO_4$·$CH_3OH$ (**2**), Cu(**L2**)$(NO_3)_2$·$2(CH_2Cl_2)$ (**3**), [Cu(**L2**)$_2$]$(ClO_4)_2$·$2(CH_2CCl_2)$ (**4**), Cu(**L2**)$Cl_2$ (**5**), [$Cu_4$(**L3**)$_2(H_2O)_2$](**L3**)$_4(ClO_4)_4$ (**6**), [Ag(**L4**)$(C_2H_5OH)$]$ClO_4$ (**7**), [Ag(**L4**)$(C_2H_5OH)$]$BF_4$ (**8**), and [Ag(**L4**)$(CH_3OH)$]$SO_3CF_3$ (**9**), were isolated from the solution reactions based on these four new ligands, respectively. **L1**, **L2**, and **L3** act as convergent ligands and bind metal ions into discrete molecular complexes. In contrast, **L4** exhibits a divergent spacer to link metal ions into one-dimensional coordination polymers. New coordination compounds were fully characterized by infrared spectroscopy, elemental analysis, and single-crystal X-ray diffraction. In addition, the luminescent and electrical conductive properties of these new compounds were investigated.

## Introduction

Owing to their potential as new functional materials, interest in self-assembled coordination polymeric and discrete complexes with specific network topologies has grown rapidly.[1−4] In this context, the design and synthesis of specific organic ligands are foundational issues, because they are some of the most important factors in determining the ultimate structures that are related to their corresponding physical and chemical properties. During past decades, a number of organic ligands, including rigid linear, semirigid, and flexible organic spacers with various topologies and coordination natures, have been designed and synthesized.[1−4]

* To whom correspondence should be addressed. Email: yubindong@sdnu.edu.cn.

(1) Recent reviews on metal−organic polymers: (a) Yaghi, O. M.; O'Keeffe, M.; Ockwig, N. W.; Chae, H. K.; Eddaoudi, M.; Kim, J. *Nature* **2003**, *423*, 706. (b) Kitagawa, S.; Kitaura, R.; Noro, S.-I. *Angew. Chem. Int. Ed.* **2004**, *43*, 2334. (c) Zaworotko, M. J.; Moulton, B. *Chem. Rev.* **2001**, *101*, 2619. (d) Eddaoudi, M.; Moler, D. B.; Li, H.; Chen, B.; Reineke, T. M.; Keeffe, M. O.; Yaghi, O. M. *Acc. Chem. Res.* **2001**, *34*, 319. (e) Constable, E. C. *Prog. Inorg. Chem.* **1994**, *42*, 67. (f) Dunbar, K. R.; Heintz, K. R. *Prog. Inorg. Chem.* **1996**, *35*, 3. (g) Whiteford, J. A.; Rachlin, E. M.; Stang, P. J. *Angew. Chem., Int. Ed. Engl.* **1996**, *35*, 2524. (h) Hagrman, P. J.; Hagrman, D.; Zubieta, J. *Angew. Chem., Int. Ed.* **1999**, *38*, 2639. (i) Blake, A. J.; Champness, N. R.; Hubberstey, P.; Li, W.-S.; Withersby, M. A.; Schröder, M. *Coord. Chem. Rev.* **1999**, *183*, 117. (j) Batten, S.; Robson, R. *Angew. Chem., Int. Ed.* **1998**, *37*, 1460. (k) Barnett, S. A.; Champness, N. R. *Coord. Chem. Rev.* **2003**, *246*, 145.

(2) (a) Gardner, G. B.; Venkataraman, D.; Moore, J. S.; Lee, S. *Nature (London)* **1995**, *374*, 792. (b) Kiang, Y.-H.; Gardner, G. B.; Lee, S.; Xu, Z. *J. Am. Chem. Soc.* **2000**, *122*, 6871. (c) Maji, T. K.; Uemura, K.; Chang, H.-C.; Matsuda, R.; Kitagawa, S. *J. Am. Chem. Soc.* **2004**, *126*, 3269. (e) Dybtsev, D. N.; Chun, H.; Yoon, S. H.; Kim, D.; Kim, K. *J. Am. Chem. Soc.* **2004**, *126*, 32. (f) Su, C.-Y.; Goforth, A. M.; Smith, M. D.; Pellechia, P. J.; zur Loye, H.-C. *J. Am. Chem. Soc.* **2004**, *126*, 3576. (g) Zhou, Y.-F.; Jiang, F.-L.; Yuan, D.-Q.; Wu, B.-L.; Wang, R.-H.; Lin, Z.-Z.; Hong, M.-C. *Angew. Chem., Int. Ed.* **2004**, *43*, 5665. (h) Zhang, J.-P.; Zheng, S.-L.; Huang, X.-C.; Chen, X.-M. *Angew. Chem., Int. Ed.* **2003**, *43*, 206. (i) Zhao, B.; Chen, X.-Y.; Cheng, P.; Liao, D.-Z.; Yan, S.-P.; Jiang, Z.-H. *J. Am. Chem. Soc.* **2004**, *126*, 15394. (j) Wu, C.-D.; Lin, W. *Angew. Chem., Int. Ed.* **2005**, *44*, 1958. (k) Kong, L.-Y.; Zhang, Z.-H.; Zhu, H.-F.; Kawaguchi, H.; Okamura, T.-a.; Doi, M.; Chu, Q.; Sun, W.-Y.; Ueyama, N. *Angew. Chem., Int. Ed.* **2005**, *44*, 4352. (l) Hanson, K.; Calin, N.; Bugaris, D.; Scancela, M.; Sevov, S. C. *J. Am. Chem. Soc.* **2004**, *126*, 10502. (m) Khlobystov, A. N.; Brett, M. T.; Blake, A. J.; Champness, N. R.; Gill, P. M. W.; O'Neill, D. P.; Teat, S. J.; Wilson, C.; Schröder, M. *J. Am. Chem. Soc.* **2003**, *125*, 6753. (n) Takaoka, K.; Kawano, M.; Tominaga, M.; Fujita, M. *Angew. Chem., Int. Ed.* **2005**, *44*, 2151.

(3) (a) Steel, P. J. *Acc. Chem. Res.* **2005**, *38*, 243. (b) Badjic, J. D.; Nelson, A.; Cantrill, S. J.; Turnbull, W. B.; Stoddart, J. F. *Acc. Chem. Res.* **2005**, *38*, 723. (c) Seidel, S. R.; Stang, P. J. *Acc. Chem. Res.* **2002**, *35*, 972. (d) MacGillivray, L. R.; Atwood, J. L. *Angew. Chem., Int. Ed.* **1999**, *38*, 1018. (e) Ockwig, N. W.; Delgado-Friedrichs, O.; O'Keeffe, M.; Yaghi, O. M. *Acc. Chem. Res.* **2005**, *38*, 176. (f) Bradshaw, D.; Claridge, J. B.; Cussen, E. J.; Prior, T. J.; Rosseinsky, M. J. *Acc. Chem. Res.* **2005**, *38*, 273.

10.1021/ic0612552 CCC: $33.50 
Published on Web 11/16/2006

Moreover, some basic principles of rational design and construction of molecular architectures based on the several classes of specific organic ligands are well established. For example, "two-dimensional cyclic nanostructures", "three-dimensional molecular cages", and "high-symmetry metal−organic clusters" have recently been proposed by Stang, Fujita, and Raymond.[5−7] There is no doubt that such ligand-directed synthetic methodology plays a very important role in the construction of the predesigned supramolecular assemblies with specific structural features. In most cases, however, molecular architectures based on self-assembly have been synthesized unintentionally. In other words, the ultimate structures often deviate from the desired ones. Thus, new organic ligands must be designed and synthesized and the reaction chemistry based on them investigated to generate a sufficiently large database from which rational design strategy based on organic spacers for specific classes of molecular assemblies can be deduced.

Recently, our research group has provided a series of bent rigid and flexible organic ligands bridged by a five-membered heterocyclic ring for the assembly of polymeric and discrete metal−organic assemblies.[8] We could imagine that the bent organic ligands, because of their variational conformation (cis, trans, or any intermediary conformations between them), would offer the possibility of the construction of frameworks with novel patterns not easily achievable by linear rigid ligands, which are widely used by chemists in the generation of coordination frameworks. This alternative ligand-directed approach did result in various new polymeric and discrete coordination complexes, some with open channels and interesting luminescent properties.[8]

As an in-depth analysis and part of our systemic investigation of self-assembly based on the bent ligands of this type, we herein present the synthesis of four new organic ligands **L1**, **L2**, **L3**, and **L4** with single and double 4- or 3-pyridinecarboxylate arms (Scheme 1) bridged by a 1,3,4-oxadiazole ring and nine new silver(I) and copper(II) coordination complexes, [Ag(**L1**)]$PF_6$·$H_3OH$ (**1**), [Ag(**L1**)]$ClO_4$·$CH_3OH$ (**2**), Cu(**L2**)$(NO_3)_2$·$2(CH_2Cl_2)$ (**3**), [Cu(**L2**)$_2$]$(ClO_4)_2$·$2(CH_2CCl_2)$ (**4**), [Cu(**L2**)]$Cl_2$ (**5**), [$Cu_4$(**L3**)$_2(H_2O)_2$](**L3**)$_4(ClO_4)_4$ (**6**), [Ag(**L4**)$(C_2H_5OH)$]$ClO_4$ (**7**), [Ag(**L4**)$(C_2H_5OH)$]$BF_4$ (**8**), and [Ag(**L4**)$(CH_3OH)$]$SO_3CF_3$ (**9**), generated from them and various silver and copper salts, as shown in Scheme 2.

## Experimental Section

**Materials and Methods.** $AgSO_3CF_3$, $AgClO_4$, $AgBF_4$, $AgPF_6$, $Cu(ClO_4)_2$, $CuCl_2$, and $Cu(NO_3)_2$ (Acros) were used as obtained without further purification. IR samples were prepared as KBr pellets, and spectra were obtained in the 400−4000 $cm^{-1}$ range using a Perkin-Elmer 1600 Fourier transform (FT) IR spectrometer. Elemental analyses were performed on a Perkin-Elmer Model 2400 analyzer. $^1$H NMR data were collected using an AM-300 spectrometer. Chemical shifts are reported in $\delta$ relative to TMS. All fluorescence measurements were carried out on a Cary Eclipse spectrofluorometer (Varian, Australia) equipped with a xenon lamp and a quartz carrier at room temperature. Thermogravimetric analyses were carried out using a TA Instrument SDT 2960 with simultaneous differential thermal analysis and thermogravimetric analysis (DTA−TGA) under flowing nitrogen at a heating rate of 10 °C/min. X-ray diffraction (XRD) patterns were obtained on a D8 ADVANCE powder XRD with Cu K$\alpha$ radiation ($\lambda$ = 1.5405 Å).

***Caution:*** *Two of the crystallization procedures involve metal perchlorate, a strong oxidizer.*

**Preparation of L1.** Triethylamine (1.1 mL, 7.8 mmol) was added with stirring to a solution of 2,5-bis(2-hydroxyphenyl)-1,3,4-oxadiazole (1.0 g, 3.9 mmol) and isonicotinoyl chloride (0.7 g, 3.9 mmol) in anhydrous $CH_2Cl_2$ (40 mL) at ambient temperature. The mixture was stirred for 6 h at ambient temperature (monitored by thin-layer chromatography (TLC)). After removal of solvent under vacuum, the residue was purified on a silica gel column using $CH_2Cl_2$/THF (30:1, v/v) as the eluent to afford **L1** as a white crystalline solid (0.7 g). Yield: 50%. Mp: 156−158 °C. IR (KBr pellet, $cm^{-1}$): 3415(m), 3129(m), 1744(vs), 1624(m), 1595(m), 1493(s), 1402(vs), 1270(vs), 1216(s), 1059(m), 751(m). $^1$H NMR (300 MHz, $CDCl_3$, 25 °C, TMS, ppm): 10.01 (s, 1H, −OH), 8.92 (d, 2H, $-C_5H_4N$), 8.27 (m, 1H, $-C_6H_4$), 8.11 (m, 2H, $-C_5H_4N$), 7.68 (t, 1H, $-C_6H_4$), 7.55 (t, 1H, $-C_6H_4$), 7.40 (t, 3H, $-C_6H_4$), 7.09 (d, 1H, $-C_6H_4$), 6.82 (t, 1H, $-C_6H_4$). Anal. Calcd for $C_{20}H_{13}N_3O_4$: C, 66.85; H, 3.62; N, 11.70. Found: C, 66.62; H, 3.78; N, 11.52.

**Preparation of L2.** Triethylamine (1.3 mL, 9.44 mmol) was added with stirring to a solution of 2,5-bis(2-hydroxyphenyl)-1,3,4-oxadiazole (0.6 g, 2.36 mmol) and nicotinoyl chloride (0.84 g, 4.72 mmol) in anhydrous $CH_2Cl_2$ (40 mL) at ambient temperature. The mixture was stirred for 8 h at ambient temperature (monitored by TLC). The precipitation was separated by filtration, washed several times with water, and vacuum-dried to afford a white crystalline soild (0.92 g). Yield: 84%. Mp: 244−247 °C. IR (KBr pellet,


(4) (a) Halper, S. R.; Cohen, S. *Inorg. Chem.* **2005**, *44*, 4139. (b) Burchell, T. J.; Puddephatt, R. J. *Inorg. Chem.* **2005**, *44*, 3718. (c) Chen, W.; Wang, J.-Y.; Chen, C.; Yue, Q.; Yuan, H.-M.; Chen, J.-S.; Wang, S.-N. *Inorg. Chem.* **2003**, *42*, 944. (d) Pan, L.; Huang, X.; Phan, H.-L. N.; Emge, T. J.; Li, J.; Wang, X. *Inorg. Chem.* **2004**, *43*, 6878. (e) Shin, D. M.; Lee, I. S.; Chung, Y. K. *Inorg. Chem.* **2003**, *42*, 8838. (f) Chen, C.-L.; Goforth, A. M.; Smith, M. D.; Su, C.-Y.; zur Loye, H.-C. *Inorg. Chem.* **2005**, *44*, 8762.

(5) (a) Kryschenko, Y. K.; Seidel, S. R.; Muddiman, D. C.; Nepomuceno, A. I.; Stang, P. J. *J. Am. Chem. Soc.* **2003**, *125*, 9647. (b) Das, N.; Mukherjee, P. S.; Arif, A. M.; Stang, P. J. *J. Am. Chem. Soc.* **2003**, *125*, 13950. (c) Mukherjee, P. S.; Das, N.; Kryschenko, Y. K.; Arif, A. M.; Stang, P. J. *J. Am. Chem. Soc.* **2004**, *126*, 2464.

(6) (a) Yamanoi, Y.; Sakamoto, Y.; Kusukawa, T.; Fujita, M.; Sakamoto, S.; Yamaguchi, K. *J. Am. Chem. Soc.* **2001**, *123*, 980. (b) Nakabayashi, K.; Kawano, M.; Yoshizawa, M.; Ohkoshi, S.-I.; Fujita, M. **2004**, *126*, 16694. (c) Tashiro, S.; Tominaga, M.; Kawano, M.; Therrien, B.; Ozeki, T.; Fujita, M. **2005**, *127*, 4546. (d) Yashizawa, M.; Nakagawa, J.; Kumazawa, K.; Nagao, M.; Kawano, M.; Ozeki, T.; Fujita, M. *Angew. Chem. Int. Ed*. **2005**, *44*, 1810.

(7) (a) Brückner, C. B.; Powers, R. E.; Raymond, K. N. *Angew. Chem., Int. Ed.* **1998**, *37*, 1837. (b) Sun, X.; Johnson, D. W.; Caulder, D. L.; Powers, R. E.; Raymond, K. N.; Wong, E. H. *Angew. Chem., Int. Ed.* **1999**, *38*, 1303. (c) Johnson, D. W.; Xu, J.; Saalfrank, R. W.; Raymond, K. N. *Angew. Chem., Int. Ed.* **1999**, *38*, 2882. (d) Xu, J.; Parac, T. N.; Raymond, K. N. *Angew. Chem., Int. Ed.* **1999**, *38*, 2878. (e) Xu, J.; Raymond, K. N. *Angew. Chem., Int. Ed.* **2000**, *39*, 2745.

(8) (a) Dong, Y.-B.; Ma, J.-P.; Huang, R.-Q.; Smith, M. D.; zur Loye, H.-C. *Inorg. Chem.* **2003**, *42*, 294. (b) Dong, Y.-B.; Cheng, J.-Y.; Wang, H.-Y.; Huang, R.-Q.; Tang, B.; Smith, M. D.; zur Loye, H.-C. *Chem. Mater*. **2003**, *15*, 2593. (c) Dong, Y.-B.; Ma, J.-P.; Huang, R.-Q.; Liang, F.-Z.; Smith, M. D. *J. Chem. Soc., Dalton Trans.* **2003**, *9*, 1472. (d) Dong, Y.-B.; Cheng, J.-Y.; Huang, R.-Q.; Tang, B.; Smith, M. D.; zur Loye, H.-C. *Inorg. Chem*. **2003**, *42*, 5699. (e) Dong, Y.-B.; Cheng, J.-Y.; Ma, J.-P.; Huang, R.-Q.; Smith, M. D. *Cryst. Growth Des.* **2005**, *5*, 585. (f) Dong, Y.-B.; Wang, H.-Y.; Ma, J.-P.; Huang, R.-Q.; Smith, M. D. *Cryst. Growth Des.* **2005**, *5*, 789. (h) Dong, Y.-B.; Wang, H.-Y.; Ma, J.-P.; Shen, D.-Z.; Huang, R.-Q. *Inorg. Chem.* **2005**, *44*, 4679. (i) Dong, Y.-B.; Zhang, Q.; Wang, L.; Ma, J.-P.; Huang, R.-Q.; Shen, D.-Z.; Chen, D.-Z. *Inorg. Chem.* **2005**, *44*, 6591. (j) Dong, Y.-B.; Xu, H.-X.; Ma, J.-P.; Huang, R.-Q. *Inorg. Chem.* **2006**, *45*, 3325.

**Scheme 1.** Synthesis of New Ligands **L1**−**L4**

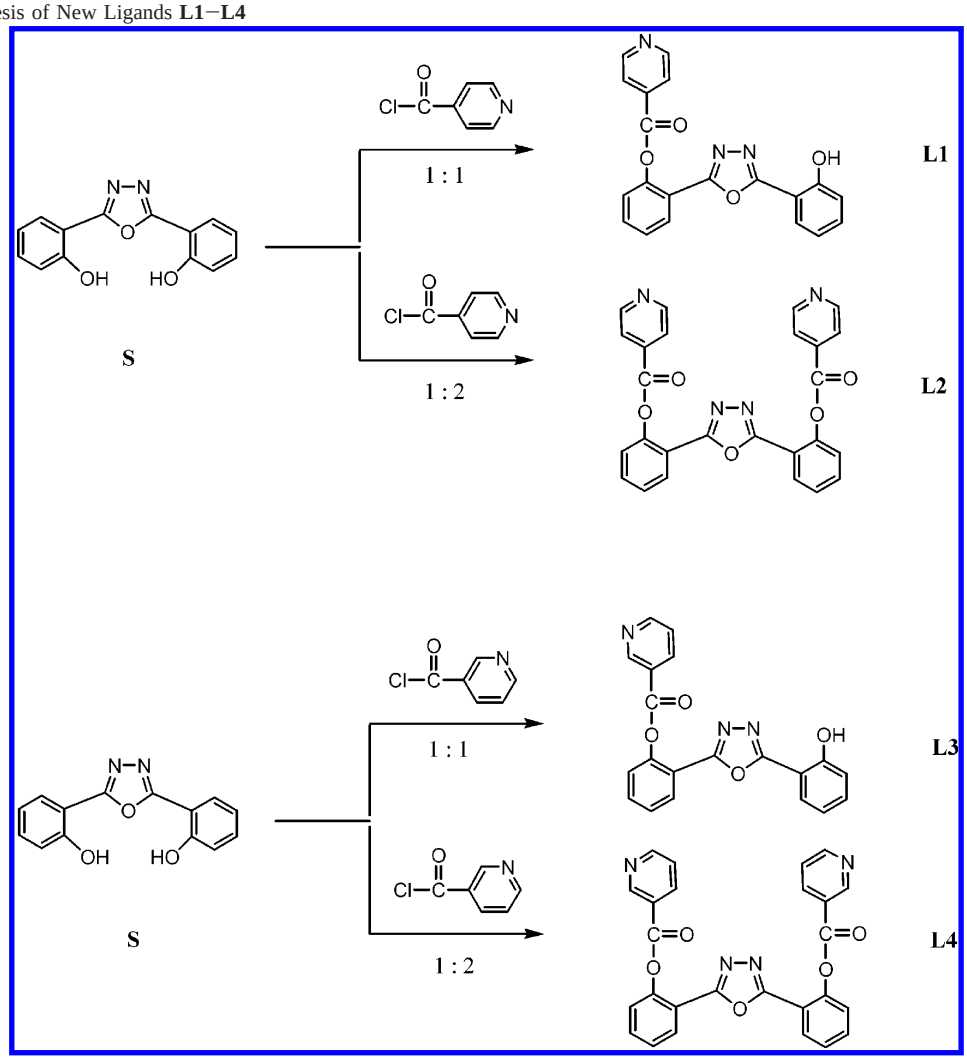


$cm^{-1}$): 3420(m), 3117(m), 1755(vs), 1611(m), 1544(m), 1496(s), 1404(s), 1277(vs), 1224(s), 1098(s), 1037(s), 776(m), 745(s), 698(s). $^1$H NMR (300 MHz, $CDCl_3$, 25 °C, TMS, ppm): 8.89 (d, 4H, $-C_5H_4N$), 8.03 (d, 4H, $-C_5H_4N$), 7.90 (d, 2H, $-C_6H_4$), 7.76 (t, 2H, $-C_6H_4$), 7.61 (d, 2H, $-C_6H_4$), 7.44(t, 2H, $-C_6H_4$). Anal. Calcd for $C_{26}H_{16}N_4O_5$: C, 67.24; H, 3.45; N, 12.07. Found: C, 67.12; H, 3.63; N, 12.15.

**Preparation of L3.** Triethylamine (1.1 mL, 7.8 mmol) was added with stirring to a solution of 2,5-bis(2-hydroxyphenyl)-1,3,4-oxadiazole (1.0 g, 3.9 mmol) and nicotinoyl chloride (0.7 g, 3.9 mmol) in anhydrous $CH_2Cl_2$ (40 mL) at ambient temperature. The mixture was stirred for 6 h at ambient temperature (monitored by TLC). After removal of solvent under vacuum, the residue was purified on a silica gel column using $CH_2Cl_2$/THF (30:1, v/v) as the eluent to afford **L3** as a white crystalline solid (0.65 g). Yield: 46%. Mp: 160−162 °C. IR (KBr pellet, $cm^{-1}$): 3412(s), 3141(s), 1742(s), 1618(vs), 1493(s), 1400(vs), 1277(s), 1209(s), 1168(m), 1059(m), 622(vs). $^1$H NMR (300 MHz, $CDCl_3$, 25 °C, TMS, ppm): 10.02 (s, 1H, −OH), 9.52 (s, 1H, $-C_5H_4N$), 8.91 (d, 1H, $-C_5H_4N$), 8.55 (d, 1H, $-C_5H_4N$), 8.25 (d, 1H, $-C_5H_4N$), 7.69 (t, 1H, $-C_6H_4$), 7.52 (m, 2H, $-C_6H_4$), 7.40 (m, 3H, $-C_6H_4$), 7.08 (d, 1H, $-C_6H_4$), 6.82 (t, 1H, $-C_6H_4$). Anal. Calcd for $C_{20}H_{13}N_3O_4$: C, 66.85; H, 3.62; N, 11.70. Found: C, 66.72; H, 3.71; N, 11.56.

**Preparation of L4.** Triethylamine (1.3 mL, 9.44 mmol) was added with stirring to a solution of 2,5-bis(2-hydroxyphenyl)-1,3,4-oxadiazole (0.6 g, 2.36 mmol) and nicotinoyl chloride (0.84 g, 4.72 mmol) in anhydrous $CH_2Cl_2$ (40 mL) at ambient temperature. The mixture was stirred for 8 h at ambient temperature (monitored by TLC). The precipitation was separated by filtration, washed several times with water, and vacuum-dried to afford a white crystalline soild (1.0 g). Yield: 91%. Mp: 232−234 °C, IR (KBr pellet, $cm^{-1}$): 3460(m), 3118(m), 1753(vs), 1611(m), 1587(s), 1547(s), 1496(s), 1420(m), 1284(vs), 1209(vs), 1088(vs), 1021(s), 851(m), 773(s), 722(s), 694(s). $^1$H NMR (300 MHz, $CDCl_3$, 25°C, TMS, ppm): 9.44 (s, 2H, $-C_5H_4N$), 8.87 (d, 2H, $-C_5H_4N$), 8.51 (d, 2H, $-C_5H_4N$), 7.83 (d, 2H, $-C_5H_4N$), 7.60 (t, 2H, $-C_6H_4$), 7.45 (m, 2H, $-C_6H_4$), 7.36 (d, 2H, $-C_6H_4$), 7.30 (d, 2H, $-C_6H_4$). Anal. Calcd for $C_{26}H_{16}N_4O_5$: C, 67.24; H, 3.45; N, 12.07. Found: C, 67.38; H, 3.21; N, 11.95.

**Preparation of [Ag(L1)]$PF_6$·$CH_3OH$ (1).** A solution of $AgPF_6$ (7.6 mg, 0.03 mmol) in MeOH (2 mL) was layered onto a solution of **L1** (10.0 mg, 0.03 mmol) in $CH_2Cl_2$ (2 mL). The solutions were left for about 2 weeks at room temperature, and colorless crystals were obtained. Yield: 79% (based on $AgPF_6$). IR (KBr pellet, $cm^{-1}$): 3514(m), 3083(m), 1749(s), 1610(s), 1537(s), 1492(s), 1271(s), 1211(s), 1062(s), 844(vs), 751(m). $^1$H NMR (300 MHz, DMSO, 25 °C, TMS, ppm): 10.22 (s, 1H, −OH), 8.89 (d, 2H, $-C_5H_4N$), 8.23 (d, 1H, $-C_6H_4$), 8.06 (d, 2H, $-C_5H_4N$), 7.77 (t, 1H, $-C_6H_4$), 7.62 (m, 3H, $-C_6H_4$), 7.40 (t, 1H, $-C_6H_4$), 7.03 (d, 1H, $-C_6H_4$), 6.86 (t, 1H, $-C_6H_4$), 4.09 (q, 1H, Me−OH), 3.15 (d, 2H, $-CH_3$). Anal. Calcd for $C_{21}H_{17}AgF_6N_3O_5P$: C, 39.13; H, 2.64; N, 6.52. Found: C, 39.25; H, 2.52; N, 6.45.

**Scheme 2.** Synthesis of New Complexes **1**−**9**

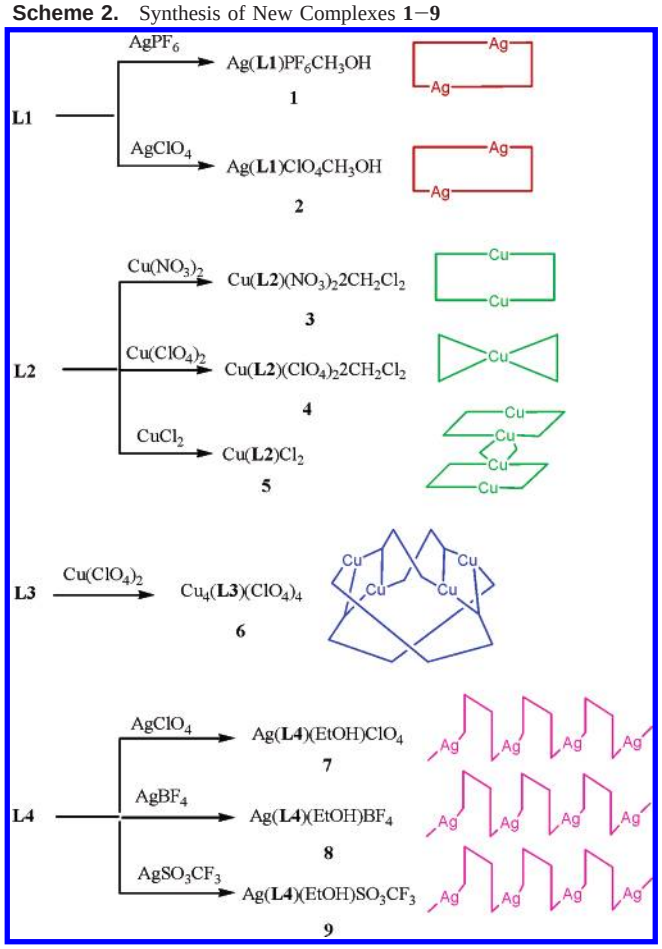


**Preparation of [Ag(L1)]$ClO_4$·$CH_3OH$ (2).** A solution of $AgClO_4$ (6.2 mg, 0.03 mmol) in MeOH (2 mL) was layered onto a solution of **L1** (10.0 mg, 0.03 mmol) in $CH_2Cl_2$ (2 mL). The solutions were left for about 2 weeks at room temperature, and colorless crystals were obtained. Yield: 82% (based on $AgClO_4$). IR (KBr pellet, $cm^{-1}$): 3462(m), 1768(s), 1610(s), 1539(s), 1492(s), 1441(m), 1271(s), 1202(s), 1085(vs), 751(m). $^1H$ NMR (300 MHz, DMSO, 25 °C, TMS, ppm): 10.22 (s, 1H, −OH), 8.89 (d, 2H, $-C_5H_4N$), 8.23 (d, 1H, $-C_6H_4$), 8.06 (d, 2H, $-C_5H_4N$), 7.77 (t, 1H, $-C_6H_4$), 7.62 (m, 3H, $-C_6H_4$), 7.40 (t, 1H, $-C_6H_4$), 7.03 (d, 1H, $-C_6H_4$), 6.86 (t, 1H, $-C_6H_4$), 4.09 (q, 1H, R−OH), 3.15 (d, 2H, $-CH_3$). Anal. Calcd for $C_{21}H_{17}AgClN_3O_9$: C, 42.14; H, 2.84; N, 7.02. Found: C, 42.01; H, 2.92; N, 7.15.

**Preparation of Cu(L2)$(NO_3)_2$·2$(CH_2Cl_2)$ (3).** A solution of $Cu(NO_3)_2$·$3H_2O$ (7.25 mg, 0.03 mol) in EtOH (8 mL) was layered onto a solution of **L2** (14.0 mg, 0.03 mmol) in $CH_2Cl_2$ (8 mL). The solutions were left for about 1 week at room temperature, and blue crystals were obtained. Yield: 72% (based on $Cu(NO_3)_2$·$3H_2O$). IR (KBr pellet, $cm^{-1}$): 3441(m), 1775(vs), 1613(s), 1493(s), 1421(s), 1384(vs), 1271(vs), 1203(s), 1091(s), 1061(s), 692(m). Anal. Calcd for $C_{28}H_{20}CuCl_4N_6O_{11}$: C, 40.87; H, 2.43; N, 10.22. Found: C, 40.22; H, 2.51; N, 10.12.

**Preparation of [Cu(L2)$_2$]$(ClO_4)_2$·2(THF) (4).** A solution of $Cu(ClO_4)_2$·$6H_2O$ (11.1 mg, 0.03 mmol) in EtOH (8 mL) was layered onto a solution of **L2** (14.0 mg, 0.03 mmol) in THF (8 mL). The solutions were left for about 2 weeks at room temperature, and purple crystals were obtained. Yield: 78% (based on $Cu(ClO_4)_2$·$6H_2O$). IR (KBr pellet, $cm^{-1}$): 3445(m), 1757(vs), 1613(m), 1492(s), 1424(m), 1269(vs), 1205(s), 1121(vs), 1091(vs), 1059(s), 684(m). Anal. Calcd for $C_{60}H_{48}CuCl_2N_8O_{20}$: C, 53.93; H, 3.59; N, 8.39. Found: C, 53.78; H, 3.72; N, 10.92.

**Preparation of Cu(L2)$Cl_2$ (5).** A solution of $CuCl_2$·$2H_2O$ (5.1 mg, 0.03 mmol) in MeOH (8 mL) was layered onto a solution of **L2** (14.0 mg, 0.03 mmol) in THF (8 mL). The solutions were left for about 2 weeks at room temperature, and green crystals were obtained. Yield: 80% (based on $CuCl_2$·$2H_2O$). IR (KBr pellet, $cm^{-1}$): 3445(m), 1752(vs), 1612(m), 1543(m), 1493(s), 1419(s), 1276(vs), 1226(s), 1210(s), 1030(m), 686(m). Anal. Calcd for $C_{26}H_{16}CuCl_2N_4O_5$: C, 52.09; H, 2.67; N, 9.35. Found: C, 52.41; H, 2.53; N, 9.42.

**Preparation of [$Cu_4$(L3)$_4$($C_4H_8O$)$_2$($H_2O$)$_2$]$(ClO_4)_4$ (6).** A solution of $Cu(ClO_4)_2$·$6H_2O$ (11.1 mg, 0.03 mmol) in EtOH (8 mL) was layered onto a solution of **L3** (10.0 mg, 0.03 mmol) in THF (8 mL). The solutions were left for about 5 days at room temperature, and green crystals were obtained. Yield: 76% (based on $Cu(ClO_4)_2$·$6H_2O$). IR (KBr pellet, $cm^{-1}$): 3441(m), 1750(s), 1608(vs), 1542(s), 1493(m), 1479(m), 1435(s), 1272(s), 1206(s), 1120(vs), 1089(vs), 774(m), 588(m). Anal. Calcd for $C_{88}H_{68}Cu_4Cl_4N_{12}O_{36}$: C, 46.60; H, 3.00; N, 7.41. Found: C, 46.48; H, 3.12; N, 7.32.

**Preparation of [Ag(L4)(EtOH)]$ClO_4$ (7).** A solution of $AgClO_4$ (4.2 mg, 0.02 mmol) in EtOH (8 mL) was layered onto a solution of **L4** (10 mg, 0.02 mmol) in THF (8 mL). The solutions were left for about 10 days at room temperature, and colorless crystals were obtained. Yield: 75% (based on $AgClO_4$). IR (KBr pellet, $cm^{-1}$): 3446(m), 1748(vs), 1610(s), 1542(m), 1494(s), 1432(m), 1275(s), 1206(s), 1092(vs), 729(m). $^1H$ NMR (300 MHz, DMSO, 25 °C, TMS, ppm): 9.27 (s, 2H, $-C_5H_4N$), 8.90 (d, 2H, $-C_5H_4N$), 8.48 (d, 2H, $-C_5H_4N$), 7.85 (d, 2H, $-C_5H_4N$), 7.72 (t, 2H, $-C_6H_4$), 7.64 (m, 2H, $-C_6H_4$), 7.57 (d, 2H, $-C_6H_4$), 7.40 (t, 2H, $-C_6H_4$). Anal. Calcd for $C_{28}H_{22}AgClN_4O_{10}$: C, 46.86; H, 3.07; N, 7.81. Found: C, 46.54; H, 3.15; N, 7.76.

**Preparation of [Ag(L4)(EtOH)]$BF_4$ (8).** A solution of $AgBF_4$ (3.9 mg, 0.02 mmol) in EtOH (8 mL) was layered onto a solution of **L4** (10 mg, 0.02 mmol) in THF (8 mL). The solutions were left for about 10 days at room temperature, and colorless crystals were obtained. Yield: 68% (based on $AgBF_4$). IR (KBr pellet, $cm^{-1}$): 3440(m), 1749(vs), 1611(s), 1543(m), 1496(s), 1431(m), 1384(m), 1275(s), 1206(s), 1084(vs), 728(m). $^1H$ NMR (300 MHz, DMSO, 25 °C, TMS, ppm): 9.28 (s, 2H, $-C_5H_4N$), 8.91 (s, 2H, $-C_5H_4N$), 8.48 (d, 2H, $-C_5H_4N$), 7.86 (d, 2H, $-C_5H_4N$), 7.72 (t, 2H, $-C_6H_4$), 7.64 (t, 2H, $-C_6H_4$), 7.58 (d, 2H, $-C_6H_4$), 7.40 (t, 2H, $-C_6H_4$). Anal. Calcd for $C_{28}H_{22}AgBF_4N_4O_6$: C, 47.73; H, 3.13; N, 7.95. Found: C, 47.58; H, 3.24; N, 8.12.

**Preparation of [Ag(L3)($CH_3OH$)]$SO_3CF_3$ (9).** A solution of $AgSO_3CF_3$ (5.2 mg, 0.02 mmol) in MeOH (8 mL) was layered onto a solution of **L4** (10 mg, 0.02 mmol) in THF (8 mL). The solutions were left for about 10 days at room temperature, and colorless crystals were obtained. Yield: 75% (based on $AgSO_3CF_3$). IR (KBr pellet, $cm^{-1}$): 3463(m), 1749(vs), 1610(s), 1542(m), 1495(s), 1432(m), 1273(vs), 1224(s), 1169(m), 1030(s), 694(m). $^1H$ NMR (300 MHz, DMSO, 25 °C, TMS, ppm): 9.28 (s, 2H, $-C_5H_4N$), 8.90 (d, 2H, $-C_5H_4N$), 8.48 (d, 2H, $-C_5H_4N$), 7.86 (d, 2H, $-C_5H_4N$), 7.73 (t, 2H, $-C_6H_4$), 7.64 (m, 2H, $-C_6H_4$), 7.58 (d, 2H, $-C_6H_4$), 7.40 (t, 2H, $-C_6H_4$). Anal. Calcd for $C_{28}H_{20}AgF_3N_4O_9S$: C, 44.62; H, 2.66; N, 7.44. Found: C, 44.52; H, 2.82; N, 7.36.

**Single-Crystal Structure Determination.** Suitable single crystals of **1**−**9** were selected and mounted in air onto thin glass fibers. X-ray intensity data were measured at 293 K on a Bruker SMART APEX CCD(charge-coupled device)-based diffractometer (Mo Kα radiation, $\lambda = 0.710\,73$ Å). The raw frame data for **1**−**9** were integrated into SHELX-format reflection files and corrected for

**Table 1.** Crystallographic Data for **L11** and **1**−**3**

| | **1** | **2** | **3** | **4** | **5** |
|---|---|---|---|---|---|
| empirical formula | $C_{21}H_{17}AgF_6N_3O_5P$ | $C_{21}H_{17}AgClN_3O_9$ | $C_{28}H_{20}Cl_4CuN_6O_{11}$ | $C_{54}H_{36}Cl_6CuN_8O_{18}$ | $C_{26}H_{16}Cl_2CuN_4O_5$ |
| fw | 644.22 | 598.70 | 821.84 | 1361.15 | 598.87 |
| cryst syst | triclinic | triclinic | triclinic | monoclinic | orthorhombic |
| *a* (Å) | 9.038(6) | 8.6858(19) | 7.2359(15) | 9.0439(10) | 8.9924(7) |
| *b* (Å) | 10.955(7) | 10.745(2) | 14.946(3) | 20.111(2) | 20.6550(14) |
| *c* (Å) | 12.219(8) | 12.457(3) | 17.339(4) | 15.6438(17) | 26.1776(19) |
| α (deg) | 86.964(9) | 87.174(3) | 111.931(4) | 90 | 90 |
| *β* (deg) | 78.308(9) | 77.727(3) | 98.549(4) | 91.563(2) | 90 |
| *γ* (deg) | 79.488(9) | 78.697(3) | 95.196(4) | 90 | 90 |
| *V* (Å$^3$) | 1164.8(13) | 1113.9(4) | 1698.2(6) | 2844.2(5) | 4862.2(6) |
| space group | $P\bar{1}$ | $P\bar{1}$ | $P\bar{1}$ | $P2_1$ | *Pnnm* |
| *Z* | 2 | 2 | 2 | 2 | 8 |
| $\rho_{calc}$ (g/cm$^3$) | 1.665 | 1.785 | 1.607 | 1.589 | 1.636 |
| $\mu$(Mo Kα) (mm$^{-1}$) | 1.022 | 1.085 | 1.025 | 0.748 | 1.166 |
| temp (K) | 293(2) | 293(2) | 293(2) | 293(2) | 293(2) |
| no. of observations ($I > 3\sigma$) | 4036 | 4058 | 6020 | 8494 | 3690 |
| final *R* indices[a] [$I > 2\sigma(I)$]: *R*; $R_w$ | 0.0534; 0.1264 | 0.0663; 0.1540 | 0.0887; 0.1532 | 0.0807; 0.1518 | 0.0920; 0.2272 |

[a] $R1 = \Sigma||F_o| - |F_c||/\Sigma|F_o|$. $wR2 = \{\Sigma[w(F_o^2 - F_c^2)^2]/\Sigma[w(F_o^2)^2]\}^{1/2}$.

**Table 2.** Crystallographic Data for **6**−**9**

| | **6** | **7** | **8** | **9** |
|---|---|---|---|---|
| empirical formula | $C_{88}H_{68}Cl_4Cu_4N_{12}O_{36}$ | $C_{28}H_{22}AgClN_4O_{10}$ | $C_{28}H_{22}AgBF_4N_4O_6$ | $C_{28}H_{20}AgF_3N_4O_9S$ |
| fw | 2265.50 | 717.82 | 705.18 | 753.41 |
| cryst syst | orthorhombic | orthorhombic | orthorhombic | monoclinic |
| *a* (Å) | 44.24(3) | 9.020(3) | 8.9908(15) | 8.995(7) |
| *b* (Å) | 19.128(14) | 10.351(4) | 10.4041(17) | 10.410(9) |
| *c* (Å) | 25.97(3) | 30.054(10) | 29.832(5) | 30.97(3) |
| α (deg) | 90 | 90 | 90 | 90 |
| *β* (deg) | 90 | 90 | 90 | 93.224(14) |
| *γ* (deg) | 90 | 90 | 90 | 90 |
| *V* (Å$^3$) | 21976(34) | 2806.2(17) | 2790.6(8) | 2896(4) |
| space group | *Fdd*2 | $P2_12_12_1$ | $P2_12_12_1$ | $P2_1/c$ |
| *Z* | 8 | 4 | 4 | 4 |
| $\rho_{calc}$ (g/cm$^3$) | 1.369 | 1.699 | 1.678 | 1.728 |
| $\mu$(Mo Kα) (mm$^{-1}$) | 0.943 | 0.880 | 0.800 | 0.850 |
| temp (K) | 293(2) | 293(2) | 293(2) | 293(2) |
| no. of observations ($I > 3\sigma$) | 7567 | 4950 | 4928 | 5047 |
| final *R* indices[a] [$I > 2\sigma(I)$]: *R*; $R_w$ | 0.0694; 0.1682 | 0.0625; 0.1079 | 0.0653; 0.1433 | 0.1086; 0.2592 |

[a] $R1 = \Sigma||F_o| - |F_c||/\Sigma|F_o|$. $wR2 = \{\Sigma[w(F_o^2 - F_c^2)^2]/\Sigma[w(F_o^2)^2]\}^{1/2}$.

**Scheme 3.** Para, Meta, and Ortho Substituted Oxadiazole-Bridged Ligands

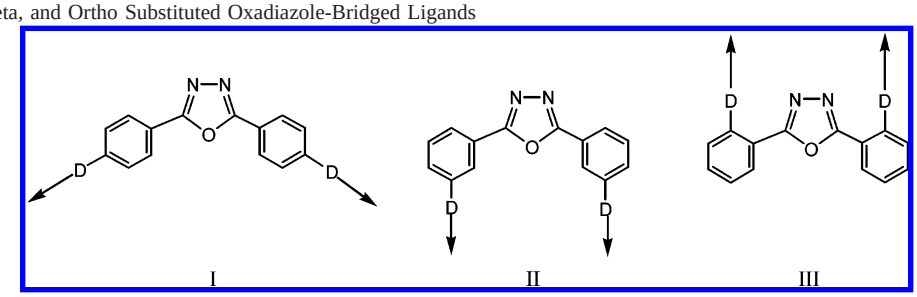


Lorentz and polarization effects using SAINT.[9] Corrections for incident and diffracted beam absorption effects were applied using SADABS.[9] None of the crystals showed evidence of crystal decay during data collection. All structures were solved by a combination of direct methods and difference Fourier syntheses and refined against $F^2$ by the full-matrix least-squares technique. Crystal data, data collection parameters, and refinement statistics for **1**−**9** are listed in Tables 1 and 2 . Relevant interatomic bond distances and bond angles for **1**−**9** are given in Tables S1−9.

(9) Bruker Analytical X-ray Systems, Inc.: Madison, WI, 1998.

## Results and Discussion

**Ligand Synthesis.** One of the important issues in determining the framework structures is the geometry of the organic ligands. In our previous study, the terminal coordinating donors are separated by the 1,3,4-oxadiazole ring at either the para (ligand I) or the meta (ligand II) positions on the phenyl rings (Scheme 3). Such a divergent arrangement would be favored to the formation of polymeric coordination polymers instead of discrete complexes. Currently, only a handful of bimetallic metallocycles have been generated

from ligand II.[8] By comparison, the convergent ligand III, with two coordination arms at the ortho positions, would be more suited for the formation of discrete complexes such as molecular rectangles, molecular boxes, or other related lower-symmetric supramolecular complexes. In addition, bulky coordination arms grafted on the 2,5-bisphenyl-1,3,4-oxadiazole backbone could result in intraligand twisting, which potentially facilitates the formation of the chiral helical structures or discrete molecular cages made up of the twist of the organic ligand. We are interested in how different types of linkages as well as differing coordinating orientations impact the structures of various metal complexes.

For a deeper understanding of the self-assembly process related to oxadiazole-bridging ligands, we designed a series of symmetric and unsymmetric organic ligands of type III. As shown in Scheme 1, **L1**, **L2**, **L3**, and **L4** were successfully synthesized by the reactions of 2,5-bis(2-hydroxylphenyl)-1,3,4-oxadiazole (**S**) with 4-pyridinecarbonyl chloride and 3-pyridinecarbonyl chloride at ambient temperature, respectively. When **S** was treated with 4- or 3-pyridinecarbonyl chloride in a 1:1 molar ratio, unsymmetric single-armed **L1** and **L2** were isolated in moderate yield; when **S** was treated with 4- or 3-pyridinecarbonyl chloride in a 1:2 molar ratio, symmetric double-armed **L3** and **L4** were generated in high yield. **L1**, **L2**, **L3**, and **L4** are soluble in common polar organic solvents such as $CH_2Cl_2$, $CHCl_3$, $CH_3CN$, and THF, which potentially facilitates the solution reaction between the ligand and inorganic metal salts. The previous study indicated that the oxadiazole ring is prone to hydrolyze into a carbohydrazide moiety when it was subjected to basic conditions.[10] The results herein demonstrate that the present oxadiazole ring is stable under our experimental conditions (triethylamine, room temperature).

**Synthesis of the Complexes.** The slow diffusion of an organic solution (THF or $CH_2Cl_2$) of new organic **L1**, **L2**, **L3**, and **L4** into a MeOH or EtOH solution of MX (M = Cu(II) and Ag(I); X = $SO_3CF_3^-$, $PF_6^-$, $ClO_4^-$, $BF_4^-$, and $Cl^-$), respectively, afforded the 1:1 metal−organic adducts with various coordination structures. Crystals formed within 0.5 month in satisfactory yield. It is worthwhile to point out that, in these specific reactions, the products do not depend on the ligand-to-metal ratio. **L1**, **L2**, and **L3** act as convergent ligands and bind metal ions into two- or three-dimensional discrete molecular complexes. Compared to **L1** and **L2**, **L3** is badly twisted in the complex. In contrast to **L1**−**L3**, **L4** herein exhibits a divergent spacer to link metal ions into one-dimensional polymeric complexes, which indicates that the different orientation of the donor groups plays a central role in determining the formation of polymer vs molecule.[11]

**Structural Analysis. Bimetallic $M_2L_2$ Rectangular Metallocycles 1 and 2 Generated from the Single-Armed L1 Ligand.** X-ray single-crystal analyses revealed that the complexes **1** and **2** form discrete bimetallic metallocycles that are composed of two **L1** ligands and two Ag(I) ions (metal-to-ligand ratio 1:1). As shown in Figure 1, each Ag(I) center adopts a $\{AgN_2O\}$ three-coordination sphere that consists of one NO-chelating donor and one pyridyl N-donor from the other **L1** ligand. Two single-armed **L1** ligands arrange in a head-to-head fashion to bind two silver atoms into a distorted rectangular binuclear ring, in which there is only one inversion center (*i*) without any crystallographically imposed symmetry for the ligands or the metal centers. In the rectangular ring, two basal 2,5-bisphenyl-1,3,4-oxadiazole moieties are strictly coplanar, but rotated by about 45° with respect to the 4-pyridinecarboxylate arms (Figure 2). Two uncoordinated EtOH molecules are hydrogen bonded to each ring through a strong O−H···O bond ($d_O$···H = 1.7 Å, $d_O$···O = 2.6 Å, ∠O−H···O = 173°).[12] Two $PF_6^-$ anions are located on both sides of the ring. In the solid state, bimetallic silver(I) macrocycles stack together along the crystallographic *b* axis by inter-ring $\pi-\pi$ (3.3 Å) interactions[13] to generate ring-containing columns (Figure 2) between which the $PF_6^-$ counterions and H-bonded EtOH molecules are located (Figure S1).

Compounds **1** and **2** are isostructural. As indicated in Figure 3, **2** adopts the same bimetallic ring as **1**. Compared to **1**, the $\pi-\pi$ stacking columns (Figure 4) and packing fashion presented in **2** are similar to those of **1**. It is noteworthy that the Ag(I) center of **2** lies in a $\{AgN_2O_2\}$ four-coordination environment, resulting from a coordinated $ClO_4^-$ anion.

The common feature of these two binuclear macrocycles lies in the fact that they are assembled from two single-armed ligands in a head-to-head fashion and two metal ions. Because the single-armed **L1** ligand is asymmetrical, the metal centers are located close to the ring corners.

**Bimetallic $M_2L_2$ Metallomacrocycles 3−5 Generated from the Double-Armed L2 Ligand.** Very recently, Stang,[5] Su, and zur Loye[14] created a new ligand-directed approach based on both organic and organometallic clips to access discrete molecular assemblies such as molecular rectangles, trigonal prisms, and many other molecular containers of varying symmetry. For the organic clip approach, the self-assembly between the designed ligand with two parallel coordination arms based on the basal organic moiety (for instance, an arene core) and di- or tricoordination acceptors. The organometallic clip methodology is based on the self-assembly of linear rigid organic spacers and di- or tricoor-

(10) (a) Lagrenée, P. M.; Sueur, S.; Wignacourt, J. P. *Acta Crystallogr.* **1991**, *C47*, 1158. (b) Incarvito, C.; Rheingold, A. L. *Inorg. Chem.* **2001**, *40*, 1386.

(11) (a) Pshirer, N. G.; Ciurtin, D. M.; Smith, M. D.; Bunz, U. H. F.; zur Loye, H.-C. *Angew. Chem., Int. Ed.* **2002**, *41*, 583. (b) Xu, Z.; Kiang, Y.-H.; Lee, S.; Lobkovsky, E. B.; Emmott, N. *J. Am. Chem. Soc.* **2000**, *122*, 8376.

(12) (a) Desiraju, G. *Acc. Chem. Res.* **2002**, *35*, 565. (b) Braga, D.; Grepioni, F. *Acc. Chem. Res.* **2000**, *33*, 601.

(13) (a) Kim, J. L.; Nilolov, D. B.; Burley, S. K. *Nature* **1993**, *365*, 520. (b) Kim, Y.; Geiger, J. H.; Hahn, S.; Sigler, P. B. *Nature (London)* **1993**, *365*, 512. (c) Guckian, K. M.; Schweitzer, B. A.; Ren, R. X.-F.; Sheils, C. J.; Tahmassebi, D. C.; Kool, E. T. *J. Am. Chem. Soc.* **2000**, *122*, 2213. (d) Fyfe, M. C. T.; Stoddart, J. F. *Acc. Chem. Res.* **1997**, *10*, 33393. (e) Ponzini, F.; Zagha, R.; Hardcastle, K.; Siegel, J. S. *Angew. Chem. Int. Ed.* **2000**, *39*, 2323.

(14) Su, C.-Y.; Cai, Y.-P.; Chen, C.-L.; Smith, M. D.; Kaim, W.; zur Loye, H.-C. *J. Am. Chem. Soc.* **2003**, *125*, 8595.

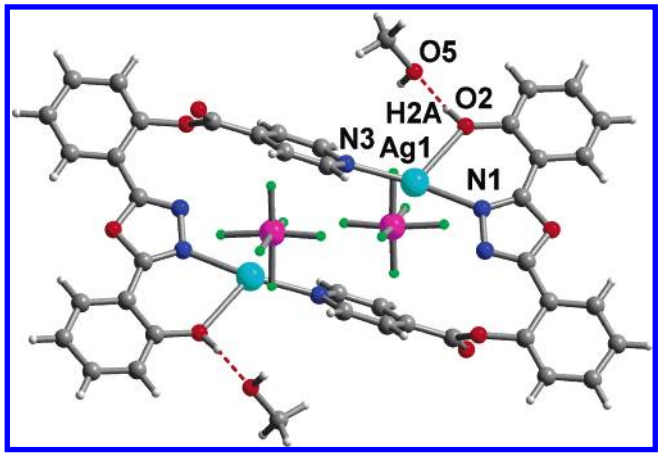


**Figure 1.** Molecular structure of **1**.

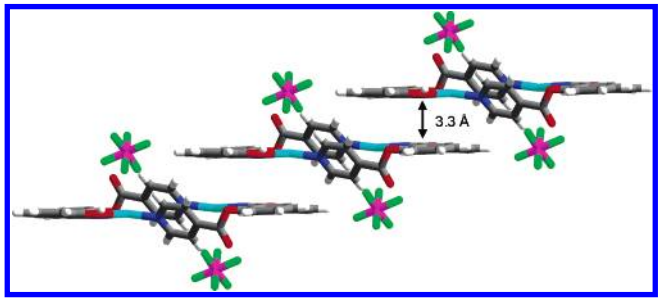


**Figure 2.** Side view of the column formed by the inter-ring $\pi-\pi$ (3.3 Å) interactions.

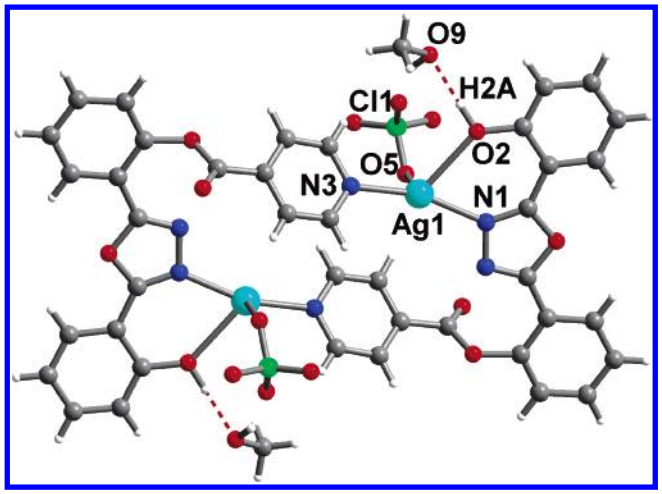


**Figure 3.** Molecular structure of **2**.

dination acceptors. By taking into account the bent geometry of five-membered heterocycle-bridging spacers, we wondered if ligand III (Scheme 3) could act as an "organic clip" to bind transition metal ions or coordination unsaturated complexes to discrete molecular assemblies. In addition, most of the known metal-coordination driven 2D and 3D discrete molecular clusters are generated from 4d and 5d metals such as Pt, Pd, Ag, and Re. In contrast, such assemblies composed of 3d metals and heterocyclic species are quite rare.[15] In principle, such heterocycle-involved metal−organic containers would promise better selectivity toward similarly shaped

(15) Mukherjee, P. S.; Min, K. S.; Arif, A. M.; Stang, P. J. *Inorg. Chem.* **2004**, *43*, 6345.

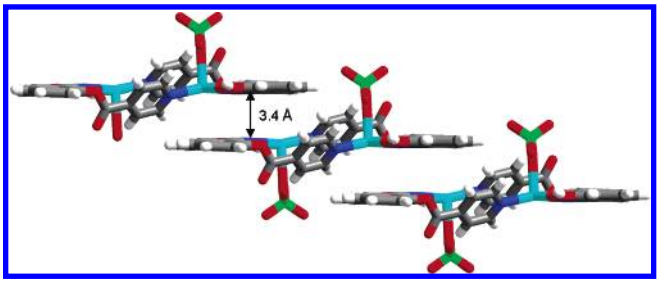


**Figure 4.** Side view of the column formed by the inter-ring $\pi-\pi$ (3.4 Å) interactions.

and functional guest molecules and are, therefore, of special interest as synthetic targets. On the other hand, 3d metal-containing discrete molecular assemblies are potentially useful in magnetic, optical, and catalytic properties. Depending on this directional bonding approach, ligand **L2** was synthesized and used as the new organic clip to bind 3d Cu(II) ion with different counterions.

Compound **3** was obtained as a discrete bimetallic complex with a rectangular-shaped structure. As indicated in Figure 5, the overall structure of **L2** is expected to be an organic clip, and two-coordination 4-pyridinecarboxylate arms are nearly parallel and point in the same direction. In addition, two 4-pyridinecarboxylate arms attached to phenyl groups are rotationally free and are thus capable of adjusting to match the metal coordination preference well. Compound **3** crystallizes in the triclinic space group, $P\bar{1}$. The copper atom lies in a $\{CuN_2O_5\}$ coordination sphere consisting of two pyridyl N-donors and five nitrate O-donors. Among five Cu−O bond distances, three Cu−O bond lengths (Cu(1)−O(9) and Cu(1)−O(7)) are in the range 2.5−2.7 Å, indicating the weak Cu−O interaction. As shown in Figure 5, two copper ions are connected by two bridging nitrate ions into a $Cu_2(NO_3)_4$ cluster. This cluster is covered by two **L2** clips from the converse directions into a molecular rectangle. The longest distance between opposite carbon atoms is 21 Å. The width, as defined by the intramolecular Cu(II)···Cu(II) distance, is 4.4 Å. As shown in Figure 5, the Cu(II) rectangle is apparently narrowed in the middle, which is caused by the two $\mu$-nitrate anions, which pulls the Cu(II) ions closer. Thus, the copper rectangle herein is strained. Moreover, the two basal 2,5-bisphenyl-1,3,4-oxadiazole backbones are coplanar, giving rise to the inter-ring $\pi-\pi$ interactions (Figure 6). Each ring stacks on its neighbors in a zigzag fashion by $\pi-\pi$ interactions extended along the crystallographic *a* axis, which generates a two-dimensional network sustained by $\pi-\pi$ contacts. The methylene chloride solvent molecules are located between these $\pi-\pi$ driven layers (Figure S2).

For studying the impact of various counterions on the self-assembly based on this type of organic clip, the weakly coordinated $ClO_4^-$ was used instead of $NO_3^-$. Crystallization of **L2** with $CuClO_4$ in the same $CH_2Cl_2$/MeOH mixed solvent system at room temperature produced compound **4** as block-like purple crystals. As indicated in Figure 7, the Cu(II) center lies in a six-coordinated 4+2 pseudooctahedral geometry defined by four pyridyl N-donors from two **L2** ligands and two oxygen atoms from two weakly coordinated

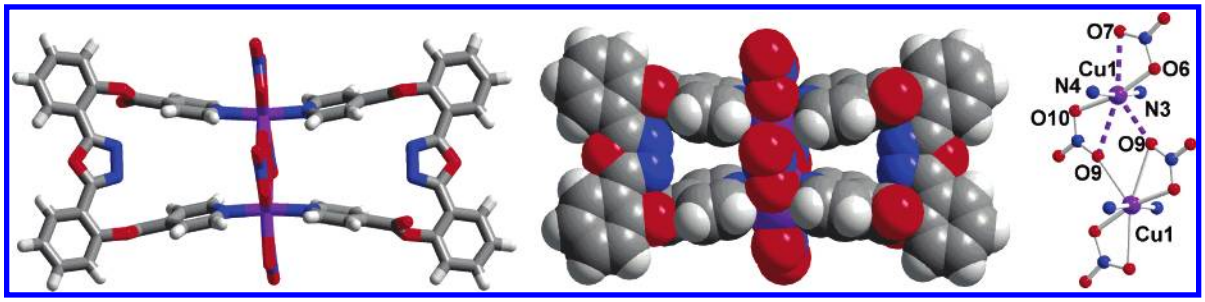


**Figure 5.** Stick (left), space-filling model (middle), and copper coordination sphere (right) of compound **3**.

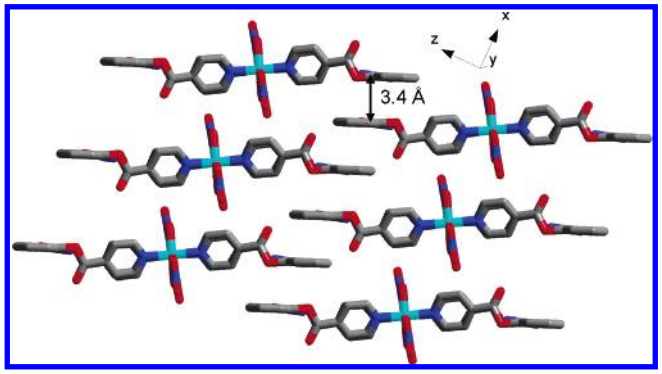


**Figure 6.** Stick and space-filling representation of the inter-ring $\pi-\pi$ (3.4 Å) interactions in **3**.

$ClO_4^-$ anions. The molecular structure of **4** is really unexpected. In **4**, the two 4-pyridinecarboxylate arms on each **L2** ligand are no longer parallel but bend markedly inward and converge at the Cu(II) intersecting point to give rise to a novel spiro-metallocycle. The dihedral angle between the phenyl ring and the attached pyridyl group is ca. 78°. Although we distance ourselves from any type of explanation and say forthright that we do not know why **4** prefers a strained cluster (being unfavorable in the self-assembly process), it is possible because of the different templating effect caused by the $ClO_4^-$ anion. Such a structural motif based on organic clips, to the best of our knowledge, has not appeared in the literature. Compound **4** shows a packing motif similar to that of **3**. As shown in Figure S3, the $\pi-\pi$ interaction driven two-dimensional net extended in the crystallographic [110] plane.

In a similar fashion, compound **5** was formed through the combination of **L2** with $CuCl_2$. X-ray single-crystal analysis revealed that there are two kinds of crystallographic Cu(II) centers in **5**. An ORTEP drawing of **5** with the atom numbering scheme is shown in Figure 8. The first Cu(II) atom resides in a distorted tetrahedral coordination sphere, $\{CuN_2Cl_2\}$, which consists of pyridyl N-donors and two chlorine atoms; the second one adopts a trigonal bipyramidal coordination sphere with the two axial positions occupied by two trans pyridyl nitrogens and the equatorial positions occupied by three chlorine atoms. It is different from **3** and **4**; two attached pyridyl groups are nearly parallel to each other but almost perpendicular to the basal 2,5-bisphenyl-1,3,4-oxadiazole plane, producing an almost regular bimetallic rectangle enclosing an internal cavity of ca. 7.4 × 14 Å (Figure 8). It is interesting that two dinuclear rectangles are connected to each other through two $\mu$-Cl ($d_{Cu(2)-Cl}$ = 2.339-(4) and 2.704(4) Å) coligands into a novel tetranuclear double macrocycle (Figure 9). Again, the inter-ring $\pi-\pi$ interactions are present because of the short $Cu_2Cl_2$ linkage and the parallel arrangement of all the 2,5-bisphenyl-1,3,4-oxadiazole moieties (Figure 10). In the solid state, tetranuclear double macrocycles stack along the crystallographic *a* axis to generate channels (Figure 10).

The common feature of compounds **3**−**5** lies in the fact that they all exhibit as the discrete macrocycles upon the "∑-shaped" conformation of **L2** ligand. As we know, the coordination behavior of 3d metal ions is versatile, and therefore, the polymeric complexes are often generated from the combination of these metal ions with organic-bridging ligands. In principle, the combination of clip-like organic ligands and metal ions would lead to both discrete rectangular and zigzag polymeric complexes. However, no oligomeric or polymeric complexes were isolated from the above reactions. Going from **3** to **5**, the distinct, different structural motifs are exhibited just by simply changing the coordination anions. Thus far, the modulation of discrete molecular architectures by changing the balance of anions remains rather uncommon.[16] In the case of the discrete closed metal−organic clusters, the counterions are rarely involved in the framework construction but are often the guest encapsulated in the host. The anion-assisting construction of discrete molecular structures affords an alternative approach to access novel molecular arrays, especially the multiloops.[17] In complexes **3**−**5**, the two attached 4-pyridinecarboxyalte arms are always located on the oxadiazole−nitrogen side and the ligand presents itself as a "∑-shaped" motif. Such a conformation is distinctly different from the 2,5-bis(3-pyridyl)-1,3,4-oxadiazole (**L**) in $M_2L_2$ (M = Zn(II), Cu(II), and Ag(I)) metal−organic clusters, where the coordination pyridyl rings reside on the oxadiazole−oxygen side and the whole ligand is shown as a "U-shaped" conformation.[8]

**Tetrametallic $M_4L_4$ Cage 6 Generated from the Single-Armed L3 Ligand.** To explore the effect of the coordinating donor orientation and molecular geometry based on this type of organic clip, we used the single-armed ligand **L3**, which possesses a 3-pyridinecarboxylate group instead of **L1**. Crystallization of the complex from $CH_2Cl_2$ and MeOH

(16) (a) Raehm, L.; Mimassi, L.; Guyard-Duhayon, C.; Amouri, H. *Inorg. Chem.* **2003**, *42*, 5654. (b) Pike, R. D.; Borne, B. D.; Maeyer, J. T.; Rheingold, A. L. *Inorg. Chem.* **2002**, *41*, 631. (c) Jung, O.-S.; Kim, Y. J.; Lee, Y.-A.; Park, K.-M.; Lee, S. S. *Inorg. Chem.* **2003**, *42*, 844. (d) Platas-lglesias, C.; Esteban, D.; Ojea, V.; Avecilla, F.; Blas, A.; Rodriguez-Blas, T. *Inorg. Chem.* **2003**, *42*, 4299. (e) Blondeau, P.; Lee, A. v.; Barboiu, M. *Inorg. Chem.* **2005**, *44*, 5649.
(17) Fujita, M. *Acc. Chem. Res.* **1999**, *32*, 53.

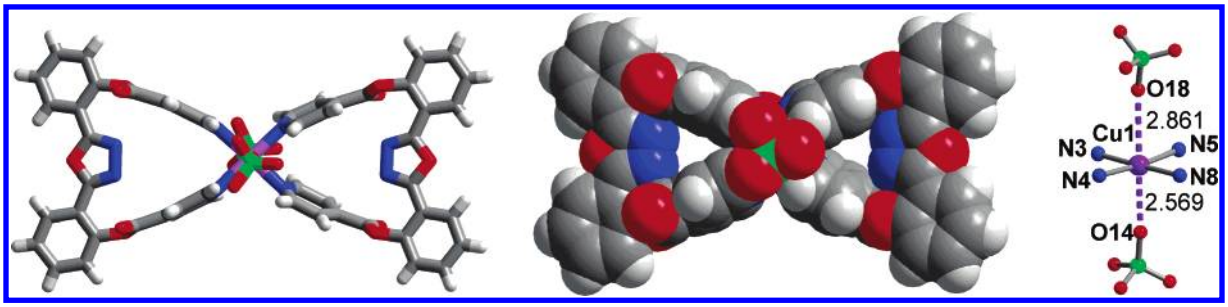


**Figure 7.** Stick (left), space-filling model (middle), and copper coordination sphere (right) of **4**.

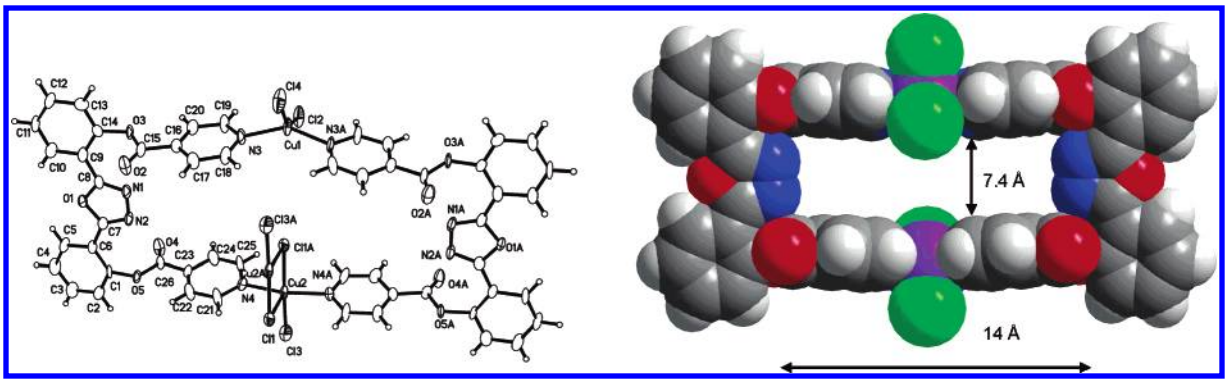


**Figure 8.** ORTEP figure and stick representation of the $Cu_2(\mathbf{L}_2)_2$ rectangle of **5**.

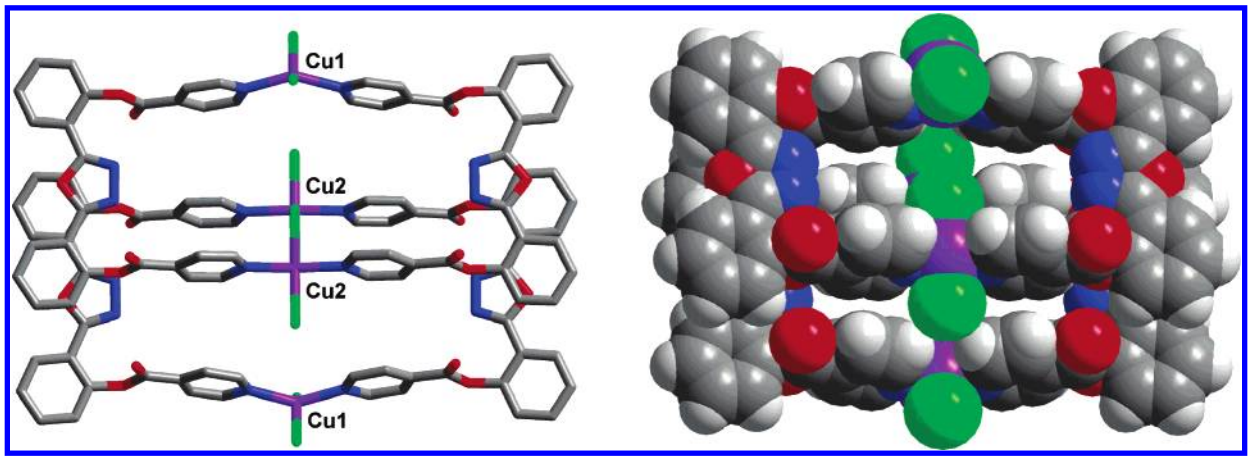


**Figure 9.** Tetranuclear double macrocycles in **5**.

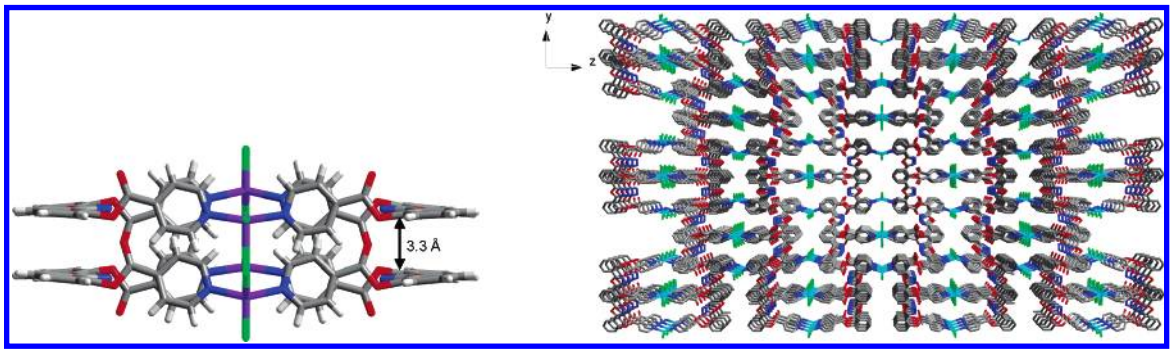


**Figure 10.** Inter-ring $\pi-\pi$ (3.3 Å) interaction in the tetranuclear double macrocycles (left) and crystal packing (right) of **5**.

afforded deep green crystals of $[Cu_4(THF)_2(H_2O)_2](\mathbf{L3})_4(ClO_4)_4$. Complex **6** crystallized in the space group *Fdd*2 with a three-dimensional cage-like structure. As shown in Figure 11, there are two different Cu(II) centers in **6**, and they all adopt a square-pyramidal coordination environment with the axial position occupied by a coordinated THF molecule (Cu(1)) and an aquo-oxygen donor (Cu(2)), respectively, and the equatorial positions occupied by one pyridyl N-donor, one oxadizole N-donor, and two hydroxyl O-donors from two **L3** ligands. The Cu−O (apical THF or $H_2O$) bond distances (2.277(11) to 2.327(9) Å) in Cu(1) and Cu(2) spheres are considerably longer than Cu−O (equatorial

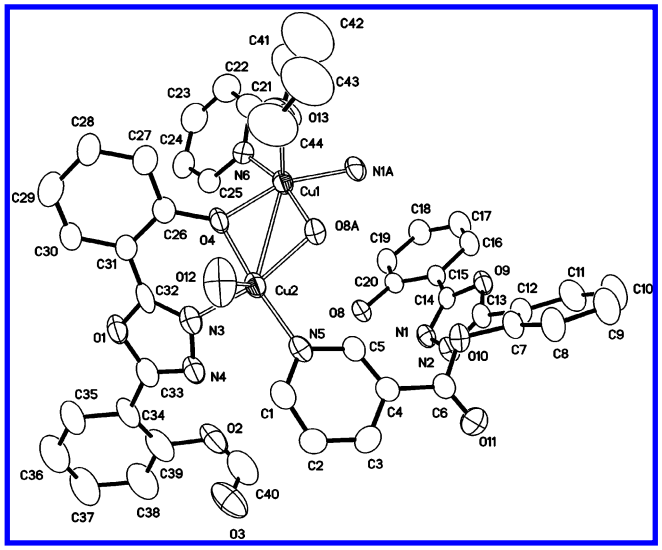


**Figure 11.** ORTEP figure of **6** (displacement ellipsoids drawn at the 30% probability level).

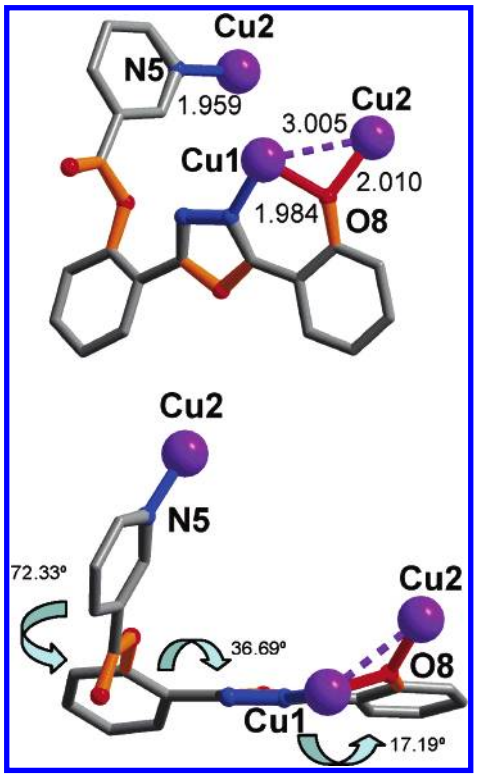


**Figure 12.** Top and side views of coordination style of **L3** in **6**.

hydroxyl group) bond lengths (1.947(7) to 2.004(8) Å)) but are within the range 2.2−2.8 Å for apical Cu−O bond distances. The **L3** ligand herein is four-coordinated and uses one pyridyl N-donor and one NO-chelating donor to bind Cu(1) and Cu(2) ions, respectively. The oxygen atom still acts as a bridging ligand to coordinate an additional Cu(2) atom, which gives rise to a short Cu(II)···Cu(II) contact of ca. 3 Å. The ligand **L3** is badly twisted, which is demonstrated by the large dihedral angles between the two phenyl and attached pyridyl groups (Figure 12).

The structure of **6** is a tetramer cage with a 3-pyridinecarboxylate arm from one monomeric unit coordinated to the next monomeric unit with the aid of the $\mu$-O-donors to finish the sphere. One uncoordinated $ClO_4^-$ anion is trapped in the pocket. When viewed down the crystallographic *a* axis (Figure 13), the hollow sphere presents a regular open rhombic section that is covered by two 3-pyridinecarboxylate linkages from the two inverse directions. The coordinated THF and $H_2O$ molecules are located outside. When viewed down the crystallographic *b* axis (Figure 13), the hollow tetrameric ball is effectively closed on both sides by $\pi-\pi$ interactions formed between two pairs of 3-pyridyl rings. In the solid state, two sets of $M_4L_4$ molecular cages arrange inversely (Figure 13).

Thus far, a large number of coordination oligomers with cyclic polygonal or polyhedral motifs have been generated on the basis of the molecular library method. The rigid symmetric organic spacers are the main theme in this context. For example, the approach for rational construction of $M_4L_4$ clusters was developed by Raymond.[7] Depending on this method, a tetrahedral $M_4L_4$ coordination cage can be achieved by the combination of a rigid $C_3$-symmetric ligand and the required metal ions. In contrast, the unsymmetric flexible ligands such as 4-pyridyl-4′-pyridylmethylenebenzene and relative analogues were often used to construct metal-catenanes.[17] To our knowledge, no $M_4L_4$ molecular cage-like complex has been synthesized on the basis of the unsymmetric single-armed flexible ligand and the metal ion, probably because of our limited understanding of how these metal−organic clusters assemble in solution from the flexible ligand and the metal component. Compound **6** herein could inspire us to design and prepare more $M_4L_4$ coordination cages exhibiting new structural features.

**One-Dimensional Polymeric Ag(I) Complexes 7−9 Based on the Double-Armed Ligand L4.** Ligand **L4** has two parallel symmetric 3-pyridinecarboxylate arms that are perpendicular to the basal 2,5-bisphenyl-1,3,4-oxadiazole to form a "Σ-shaped" spacer. It is different from **L2**; in **L4**, the two pyridyl N-donors face the opposite direction. Thus, **L4** acts as a divergent ligand. In contrast, it is well-known that the Ag(I) ion prefers a linear, "T-shaped", or trigonal coordination, geometry.[18] Thus, **L4** and Ag(I) can be employed as the angular directional components and arrange alternatively to give rise to the helical skeleton, which could be considered as an alternative rational approach to access to helical metal−organic polymers.[18b]

Crystallization of **L4** with $AgBF_4$ in the $CH_2Cl_2$/EtOH mixed solvent system at room temperature generated a chiral polymeric complex (orthorhombic, $P2_12_12_1$) with an infinite one-dimensional helical chain in high yield. In **7**, the Ag(I) center adopts a three-coordination sphere consisting of two pyridyl N-donors (Ag(1)−N(4)#1 = 2.170(8) and Ag(1)−N(3) = 2.175(8) Å) and an O-donor from a coordinated EtOH molecule with a long Ag−O bond length (Ag(1)−O(6) = 2.519(11) Å). As shown in Figure 14, the N(4)#1−Ag(1)−N(3) (155.2(3)°) angle deviates from linearity, which results in a trigonal coordination distorted toward a "T-

(18) (a) Carlucci, L. C.; Ciani, G.; Gudenberg, D. W. V.; Proserpio, D. M. *Inorg. Chem.* **1997**, *36*, 3812. (b) Jung, O.-K.; Kim, Y. J.; Lee, Y.-A.; Park, J. K.; Chae, H. K. *J. Am. Chem. Soc.* **2000**, *122*, 9921.

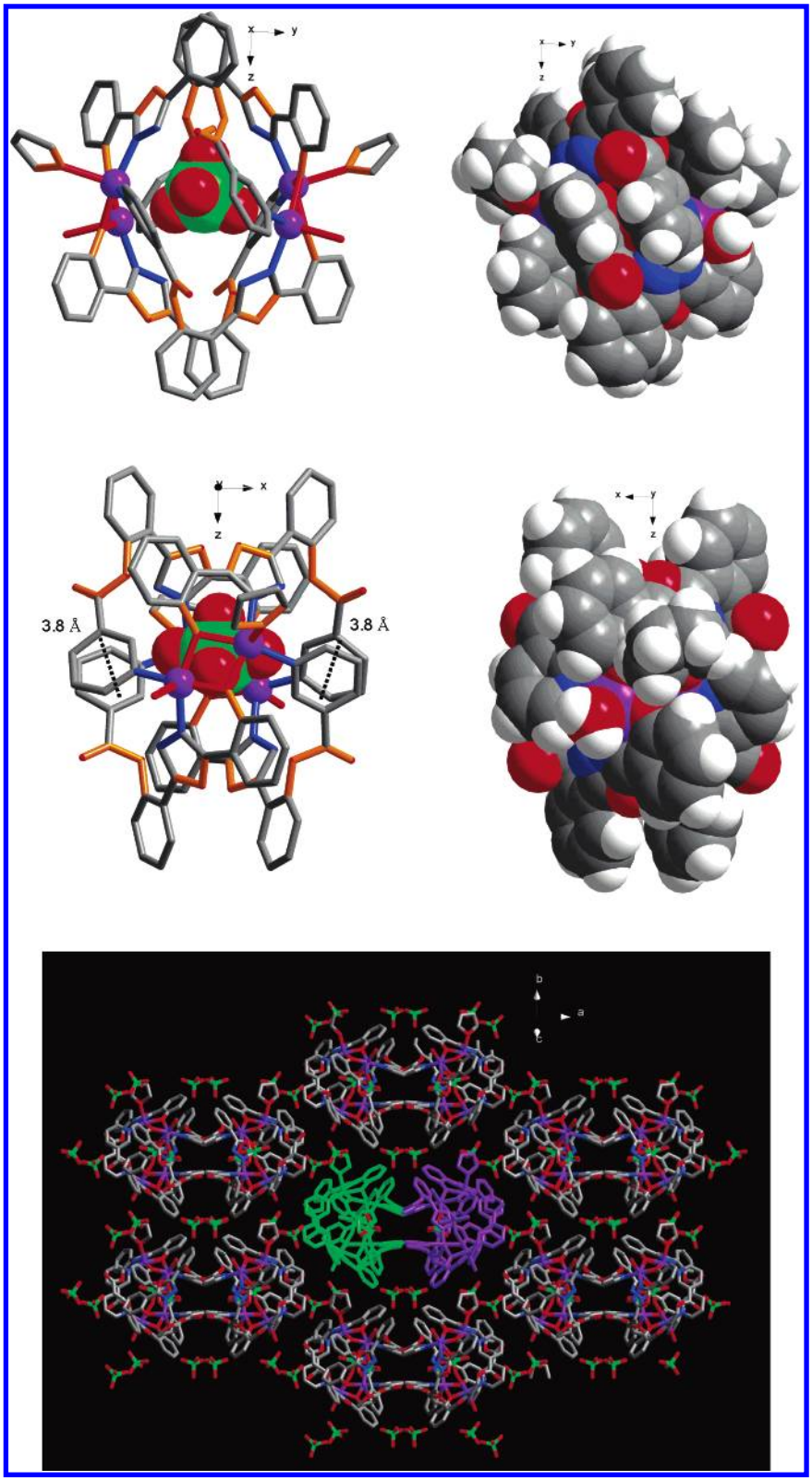


**Figure 13.** Views of the copper tetramer cage of **6** (viewed down *a* axis (top) and *b* axis (middle)) and crystal packing in the solid state. Two sets of $M_4L_4$ cages arranged in reverse (bottom).

shaped" geometry. As shown in Figure 15, the Ag(I) ions are bridged by the "Σ-shaped" **L4** ligands to form a one-dimensional helical chain along the crystallographic *b* axis, and each Ag(I) ion has a coordinated EtOH molecule. The helix consists of a right-handed single strand of alternating silver(I) and the **L4** ligand, and there is one of these units in each turn ($2_1$ along the *b* axis). The period of the helix and the translation vector in the column is equal to the crystallographic *b* axis (10.404 Å). The packing diagram reveals that the coordination polymers are more than simple helical

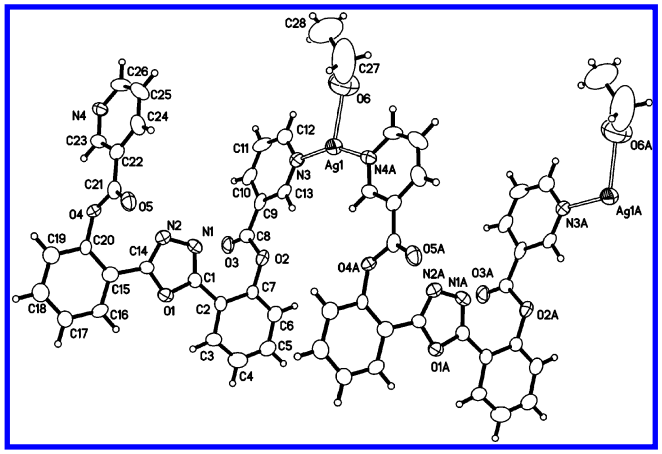


**Figure 14.** ORTEP figure of **7** (displacement ellipsoids drawn at the 30% probability level).

chains; the strands arrange as a pair of zipper-like double helices.[19] As indicated in Figure 16, two right-handed single strands are offset by one-half of a pitch along the crystallographic *b* axis and intertwine together to generate a right-handed double-stranded helix through two sets of interchain $\pi-\pi$ interactions between the oxadiazole−phenyl and phenyl−phenyl pairs. The face-to-face distances are 3.4 and 4.0 Å, respectively. Figure 17 shows that the $BF_4^-$ counterions are located between the double-stranded helical chains and they are linked together through the weak hydrogen bonding system.[20] Every two sets of H-bonds extend along the crystallographic [101] direction. The F(3)···H(3) and F(4)···H(5) distances are 2.570(5) and 2.417(6) Å, respectively. The corresponding F(3)···C(3) and F(4)···C(5) distances are 3.4 and 3.3 Å, respectively, and the corresponding F(3)···H(3)−C(3) and F(4)···H(5)−C(5) angles are 157° and 167°, respectively. Thus, the cooperation of interchain H-bonding with $\pi-\pi$ interchain interactions gives rise to the formation of the two-dimensional layers parallel to the crystallographic *ac* plane.

Compound **8** was obtained by the combination of **L4** and $AgClO_4$ under the same reaction conditions as that of **7**. Compounds **7** and **8** are isostructural. As shown in Figure 18, it possesses the same trigonally coordinated Ag(I) center and "∑-shaped" **L4** spacers, and moreover, it features the same right-handed double-stranded zipper-like helical chain in the solid state.

To explore the templating effect of the counterion and solvent molecule on the long range order of the Ag(I)−**L4** coordination polymer, the larger and polar $SO_3CF_3^-$ anion was used instead of the $BF_4^-$ and $ClO_4^-$ anions. Crystallization of **L4** with $AgSO_3CF_3$ in a mixed methanol/methylene chloride solvent system at room temperature produced the infinite noninterpenetrating two-dimensional polymeric compound **9** as block-like colorless crystals in 75% yield. Compared to **7** and **8**, **9** adopts an achiral space group (monoclinic, $P2_1/c$). As shown in Figure 19, the silver(I) atom lies in a trigonal coordination environment (Ag(1)−N(4) = 2.138(10) Å; Ag(1)−N(3) = 2.188(10) Å; Ag(1)−O(6) = 2.479(12) Å; N(4)−Ag(1)−N(3) = 154.9(4)°), which is similar to those of **7** and **8**. Again, the silver(I) centers are bridged by the **L4** ligands through the terminal pyridyl N-donors to generate the helical chains running along the crystallographic *b* axis. It is different from **7** and **8** in that **9** consists of both *M*- and *P*-configured helical chains resulting from the existing *R*- and *S*-configured **L4** ligands. As shown in Figure 20a, right- and left-handed chains arrange alternatively in the solid state. The uncoordinated $SO_3CF_3^-$ counterions are located between the right- and left-handed chains and link them together through two sets of H···F−C bonds into a one-dimensional ladder-like chain (Figure 20b,c). The F(1)···H(25) and F(3)···H(25) distances are 2.617 and 2.552 Å, and F(1)···C(25) and F(3)···C(25) are 3.1 and 3.2 Å, respectively. The corresponding ∠F(1)···H(25)···C(25) and ∠F(3)···H(25)···C(25) are 127° and 129°, respectively. Moreover, these one-dimensional chains intertwine together by two sets of interchain $\pi-\pi$ interactions (phenyl···phenyl and oxadiazole···phenyl groups) into two-dimensional nets. The corresponding face-to-face separations are 4.0 and 3.4 Å, respectively (Figure 21).

It is well-known that metal−organic helicates have played an important role in supramolecular chemistry for many years. Such materials are being used in luminescence, DNA binding, chirality, magnetic exchange, anion binding, and electrochemical structural rearrangement. In this context, the combination of the linear or bent organic ligands with suitable metal ions is demonstrated as a reliable synthetic approach. So far, various organic ligands have been used for molecular helical building blocks, but exploitation of the "∑-shaped" **L4** as a helical component has until recently remained unprecedented. The result herein demonstrates that the divergent "∑-shaped" organic spacers together with linear or trigonal metal nodes are very useful synthetic routes to metal−organic helicates. At this stage, we could not explain the achirality-forming mechanism of **9** by simply changing $BF_4^-$ in **7** and $ClO_4^-$ in **8** to $SO_3CF_3^-$ in **9**. Nevertheless, compounds **7**−**9** illustrate that the molecular construction via self-assembly is delicately dependent upon the nature of the counterions.

**Luminescent Properties of L1−L4 and Their Complexes 1−9.** Inorganic−organic hybrid coordination polymers have been investigated for fluorescence properties and for potential applications as luminescent materials, such as light-emitting diodes (LEDs).[21] Owing to the higher thermal stability of inorganic−organic coordination polymers and the ability of affecting the emission wavelength of organic materials, syntheses of inorganic−organic coordination polymers by the judicious choice of conjugated organic spacers and transition metal centers can be an efficient method for obtaining new types of electroluminescent

(19) Chen, X.-M.; Liu, G.-F. *Chem.—Eur. J.* **2002**, *8*, 4811.
(20) (a) Desirju, G. R. *Acc. Chem. Res.* **1996**, *29*, 441. (b) Dong, Y.-B.; Smith, M. D.; Layland, R. C.; zur Loye, H.-C. *Inorg. Chem.* **1999**, *38*, 5027.
(21) (a) Ciurtin, D. M.; Pschirer, N. G.; Smith, M. D.; Bunz, U. H. F.; zur Loye, H.-C. *Chem. Mater.* **2001**, *13*, 2743. (b) Cariati, E.; Bu, X.; Ford, P. C.; *Chem. Mater.* **2000**, *12*, 3385. (c) Würthner, F.; Sautter, A. *Chem. Commun.* **2000**, 445.

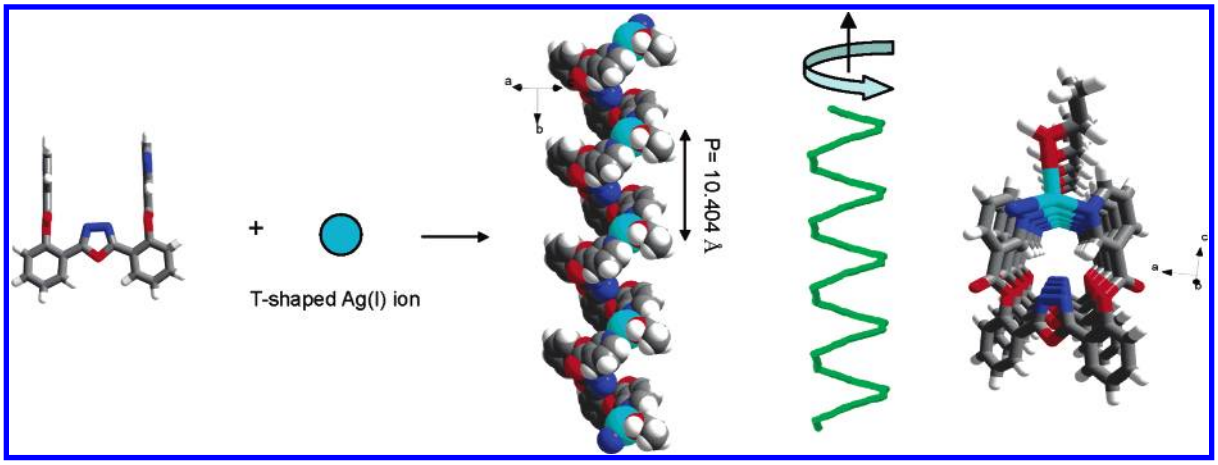


**Figure 15.** Design for the molecular helical chain from a combination of the silver(I) ion and the "Σ-shaped" spacer (side and top views).

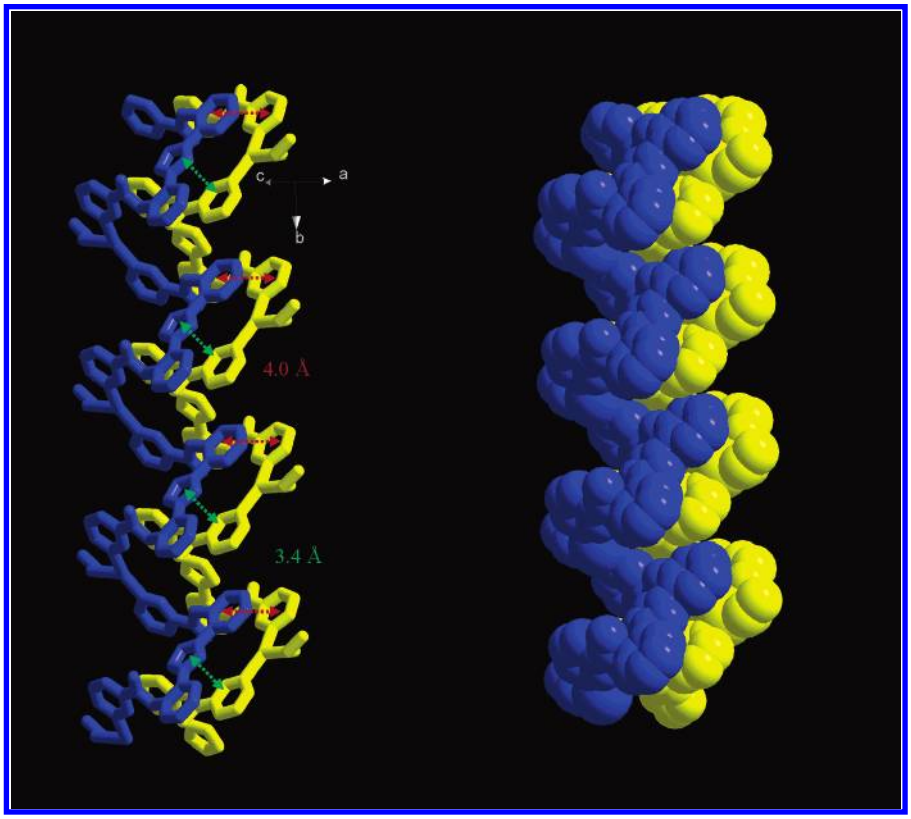


**Figure 16.** Stick (left) and space-filling (right) representation of the double-stranded helix generated by the intertwining of two single helical chains through the interchain $\pi-\pi$ interactions.

materials, especially for $d^{10}$ or $d^{10}-d^{10}$ systems[22] and oxadiazole-containing complexes.[23] We have been exploring the luminescent properties of oxadiazole-bridging organic ligands and their coordination polymers and supramolecular complexes in the solid state. The results indicate that the emission colors of these organic molecules were affected by their incorporation into metal-containing coordination compounds.[8] The luminescent properties of **L1**−**L4** and polymeric compounds **1**−**9** were investigated in the solid state. The fluorescence spectral data of **L1**−**L4** and their complexes are summarized in Table 3. In the solid state, **L1**−**L4** exhibit intense photoluminescence with an emission maximum in the range of 531, 523, 509, and 506 nm upon excitation at 351, 339, 338, and 333 nm, respectively (Figure S4). As shown in Table 3, in the solid state, the emission color of the free ligand was significantly affected by its

(22) (a) Harvey, P. D.; Gray, H. B. *J. Am. Chem. Soc.* **1988**, *110*, 2145. (b) Catalano, V. J.; Kar, H. M.; Bennett, B. L. *Inorg. Chem.* **2000**, *39*, 121. (c) Tong, M.-L.; Chen, X.-M.; Ye, B.-H.; Ji, L.-N. *Angew. Chem., Int. Ed.* **1999**, *38*, 2237. (d) Burini, A.; Bravi, R., Jr.; J. P. F.; Galassi, R.; Grant, T. A.; Omary, M. A.; Pietroni, B. R.; Staples, R. J. *Inorg. Chem.* **2000**, *39*, 3158. (e) Seward, C.; Jia, W.-L.; Wang, R.-Y.; Enright, G. D.; Wang, S.-N. *Angew. Chem., Int. Ed.* **2004**, *43*, 2933. (f) Yam, V. W.-W.; Lo, K. K.-W. *Chem. Soc. Rev.* **1999**, *28*, 323. (g) Wu, C.-D.; Ngo, H. L.; Lin, W. *Chem. Commun.* **2004**, 1588.

(23) (a) Hu, N.-X.; Esteghamatian, M.; Xie, S.; Popovic, Z.; Hor, A.-M.; Ong, B.; Wang, S.-N. *Adv. Mater.* **1999**, *11*, 1460. (b) de Silva, A. S.; de Silva, M. A. A.; Carvalho, C. E. M.; Antunes, O. A. C.; Herrera, J. O. M.; Brinn, I. M.; Mangrich, A. S. *Inorg. Chim. Acta* **1999**, *292*, 1. (c) Wang, J.; Wang, R.; Yang, J.; Zheng, Z.; Carducci, M. D.; Cayou, T.; Peyghambarian, N.; Jabbour, G. E. *J. Am. Chem. Soc.* **2001**, *123*, 6179.

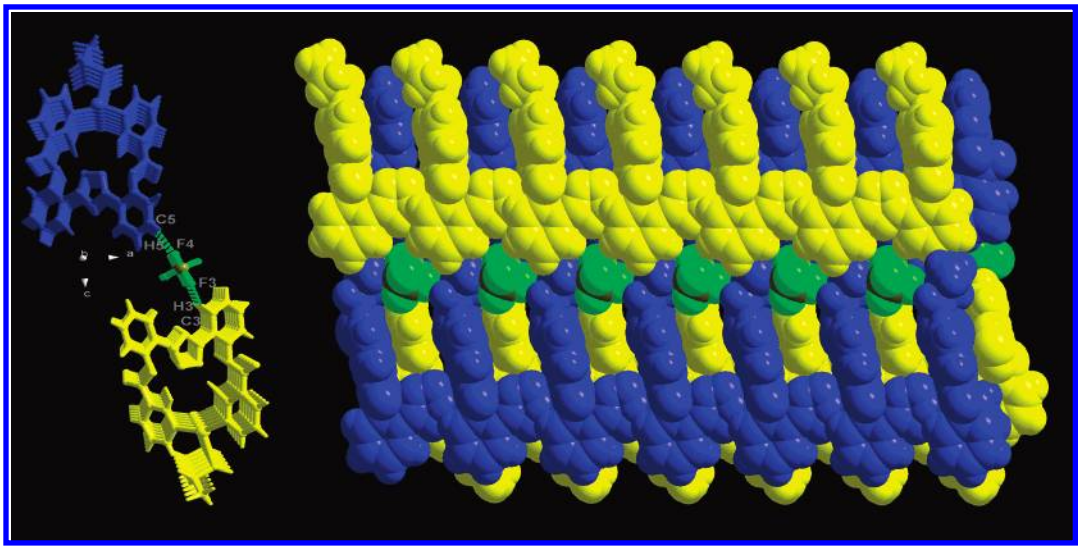


**Figure 17.** H-bonding system and crystal packing of **7**.

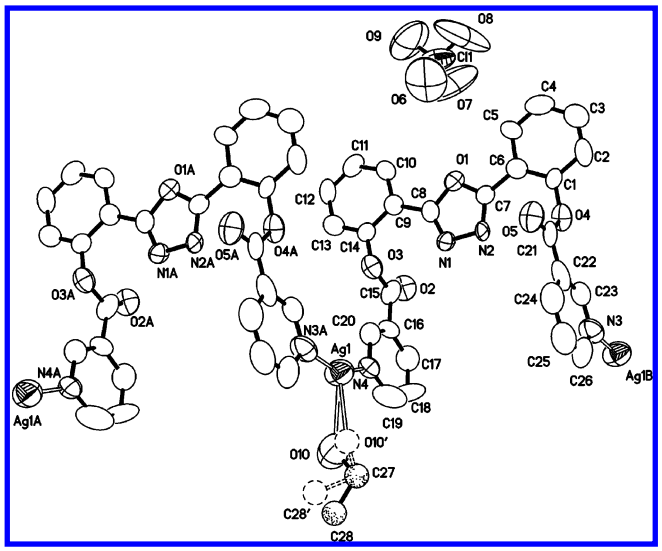


**Figure 18.** ORTEP figure of **8** (displacement ellipsoids drawn at the 30% probability level).

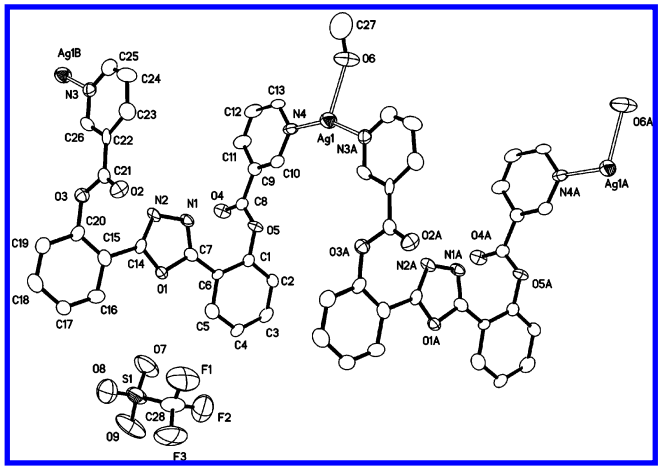


**Figure 19.** ORTEP figure of **9** (displacement ellipsoids drawn at the 30% probability level).

incorporation into the metal-containing polymeric complexes, as evidenced by the large blue shift (74−102 nm) for **1**, **2**, and **5** in the emission and red shift (32−176 nm) for **3**, **4**, **6**, and **7**−**9**, respectively. In $CH_3CN$, the emission colors between ligands **L1** and **L4** and their silver complexes are almost identical, which implies that the silver complexes disaggregate into starting materials in acetonitrile.

**Table 3.** Luminescent Properties of **L1**−**L4** and Complexes **1**−**9** in the Solid State

| compound | solid state ($\lambda_{ex}/\lambda_{em}$) | compound | solid state ($\lambda_{ex}/\lambda_{em}$) | compound | solid state ($\lambda_{ex}/\lambda_{em}$) |
|---|---|---|---|---|---|
| **L1** | 351/531 | **1** | 356/431 | **5** | 358/449 |
| **L2** | 339/523 | **2** | 355/421 | **6** | 379/685 |
| **L3** | 338/509 | **3** | 377/681 | **7** | 342/540 |
| **L4** | 333/506 | **4** | 377/679 | **8** | 341/543 |
| | | | | **9** | 341/538 |

**Electrical Conductivity.** Synthesis of single-component molecular coordination complexes by the judicious choice of organic spacers and metal centers can be an efficient method for obtaining new types of conductive materials,[24] for example, $[M(dimt)_2]_2$-type molecular complexes (M = Ni(II), Pd(II), Pt(II), Cu(II), and so on; dimt = 4,5-dimercapto-1,3-dithiole-2-thione).[25] Some of them have been confirmed to be semiconductors or superconductors. Currently, a number of molecular-based transition metal complexes with interesting electrical conductivity have been reported. However, the study of conductivity properties on polymeric coordination complexes has received considerably less attention. To explore the electrical conductivity properties of these new polymeric complexes, the electrical conductivity experiments were performed on compounds **2, 5**, and **7** in the solid state. The conductivity measurements of **2**, **4**, and **6** were performed on single crystals. The single crystal was fixed between a gold plate (10 × 4 × 1 mm) and a thin gold wire (0.2 mm in diameter, which is smaller than those of single crystals) on a piece of organic glass using gold paste. The two gold wires that extended from these two electrodes were connected to Agilent Technologies (4294A-ATO-20150). The scan range 5 ± 0.1 MHz was chosen

(24) (a) Kobayashi, A.; Tanaka, H.; Kobayashi, H. *J. Mater. Chem.* **2001**, *11*, 2078. (b) Zheng, S.-L.; Zhang, J.-P.; Wang, W.-T.; Chen, X.-M. *J. Am. Chem. Soc.* **2003**, *125*, 6882.
(25) Bousseau, M.; Valade, L.; Legros, J.-P.; Cassoux, P.; Garbauskas, M.; Interrante, V. *J. Am. Chem. Soc.* **1986**, *108*, 1908.

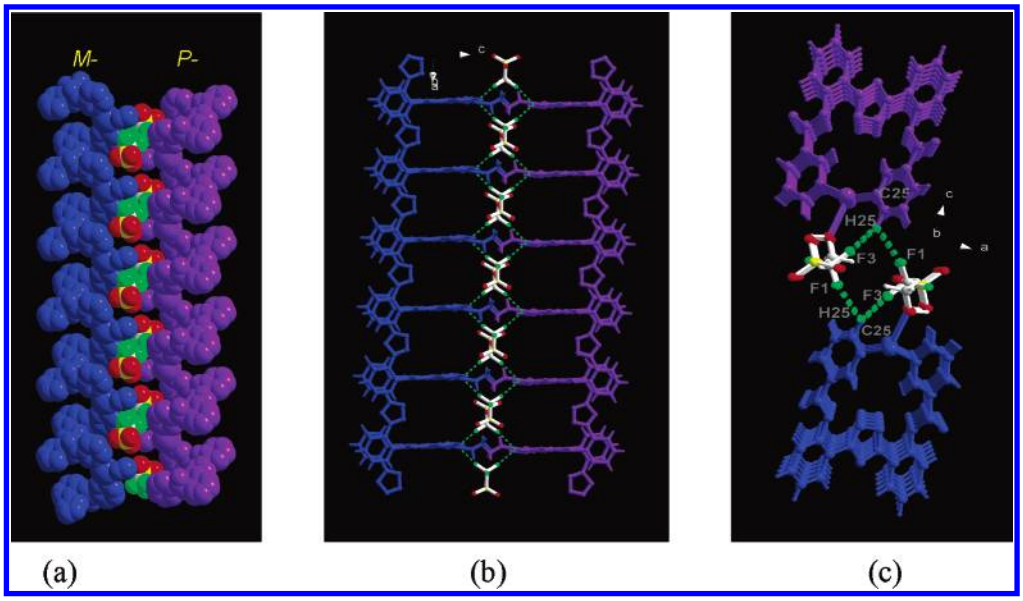


**Figure 20.** (a) Space-filling of *M*- and *P*-configured chains. The $SO_3CF_3^-$ anions are located between chains. (b) H-bonded ladder-like chain. The hydrogen bonds are shown as dotted lines. (c) H-bonding system in **9**.

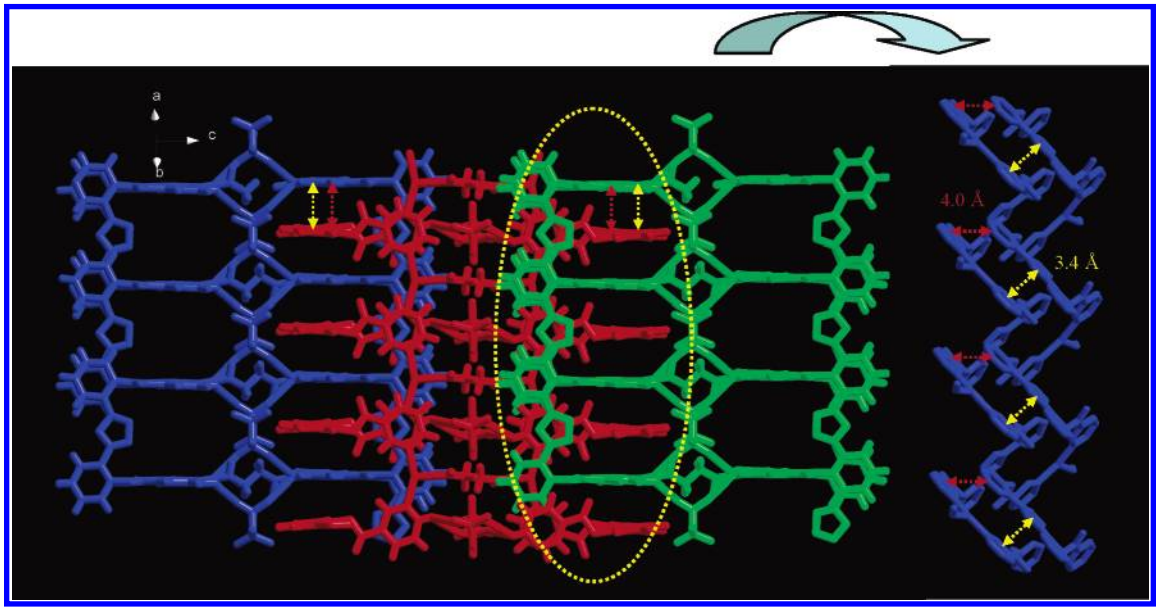


**Figure 21.** Solid-state packing of **9**. Three one-dimensional ladder-like chains are colored as blue, red, and purple, respectively (left). The $\pi-\pi$ interaction systems found in **9** (right).

**Table 4.** Electrical Conductivity of Compounds **2**, **4**, and **6**[a]

| compound | $L$ ($\mu$m) | $G$ (ns) | $B$ ($\mu$s) | $r$ ($\times 10^{-5}\ \Omega^{-1}\cdot cm^{-1}$) | $\rho$ ($\times 10^2\ \Omega\cdot m$) | $\epsilon_r$ ($\times 10^2$) |
|---|---|---|---|---|---|---|
| **2** | 0.061 | 8.1769 | 1.7639 | 0.13 | 7.71 | 1.01 |
| **4** | 0.092 | 9.9297 | 2.0332 | 0.24 | 4.21 | 1.75 |
| **6** | 0.209 | 11.4053 | 2.2896 | 0.62 | 1.61 | 4.47 |

[a] The resistivity ($\rho$) of **2**, **4**, and **6** were obtained depending on the formula $S/L\cdot G$ ($S = \pi r^2$, $L$ = length of the single crystals); dielectric constants ($\epsilon_r$) of **2**, **4**, and **6** were obtained depending on the formula of $BL/2\pi fs$.

during the measurement. The conductance ($G$) and susceptance ($B$) values were obtained on the basis of a total of 401 scanning dots. The resistivity ($\rho$) of the complexes was obtained depending on the formula $S/L\cdot G$ ($S = \pi r^2$, $L$ = length of the single crystals). The dielectric constants ($\epsilon_r$) of the complexes were obtained depending on the formula $BL/2\pi fs$. The primary result indicates that the metal−organic complexes **2**, **4**, and **6** behave as typical semiconductors with a resistivity ($\rho$) value lying in the range $1.61 \times 10^2-7.71 \times 10^2\ \Omega\cdot m$ (Table 4). The corresponding dielectric constants ($\epsilon_r$) of **2**, **4**, and **6** were obtained in the range $1.0 \times 10^2-4.47 \times 10^2$ .

## Conclusions

In conclusion, four oxadiazole-bridging ligands **L1**−**L4** with single or double pyridinecarboxylate arms were designed and synthesized by the reactions of 2,5-bis(2-hydroxylphenyl)-1,3,4-oxadiazole with 4-pyridinecarbonyl

chloride and 3-pyridinecarbonyl chloride at ambient temperature, respectively. Nine silver and copper discrete and polymeric coordination complexes have been successfully prepared by the reaction of these new ligands with various silver and copper salts in solution. This study demonstrates that the single- and double-armed oxadiazole-bridged organic ligands are useful building blocks in the construction of discrete and polymeric complexes. In addition, the different donor orientation of the ligands and the power of anion templation are the key factors in determining the final structure of a supramolecular species: for example, with the convergent ligand **L2** and the coordinating $NO_3^-$ or $Cl^-$ ions, discrete dinuclear macrocycles or tetranuclear double copper(II) macrocycles are formed, whereas, with the weakly coordinating anion $ClO_4^-$, a spiro-metallocycle is created. In contrast, the convergent ligand **L4** with silver(I) ions results in helical one-dimensional polymers. The self-assembly of the symmetric and unsymmetric bent organic ligands with rigid sidearms connected by a centrally coordinated heterocyclic ring and metal ions is a new approach to access to the discrete metallo−macrocyclic or chiral polymeric complexes. We are currently extending this result by preparing new symmetric and unsymmetric five-membered heterocyclic ring-bridging ligands of this type containing different terminal coordination functional groups. The new metal−organic polymers and supramolecular complexes based on these new bent spacers of this type with novel polymeric patterns and properties will be reported in the future.

**Acknowledgment.** We are grateful for financial support from the National Natural Science Foundation of China (nos. 20671060 and 20371030) and the Shangdong Natural Science Foundation (nos. Z2004B01 and J06D05).

**Supporting Information Available:** Crystal packing of **1**, **3**, and **4**; photo-induced emission spectra of **L1**−**L4** and **8** in the solid state; and interatomic distances and bond angles for **1**−**9**. Crystallographic data in cif format. This material is available free of charge via the Internet at http://pubs.acs.org.

IC0612552